

Hieros: Hierarchical Imagination on Structured State Space Sequence World Models

Anonymous Authors¹

Abstract

One of the biggest challenges to modern deep reinforcement learning (DRL) algorithms is sample efficiency. Many approaches learn a world model in order to train an agent entirely in imagination, eliminating the need for direct environment interaction during training. However, these methods often suffer from either a lack of imagination accuracy, exploration capabilities, or runtime efficiency. We propose HIEROS, a hierarchical policy that learns time abstracted world representations and imagines trajectories at multiple time scales in latent space. HIEROS uses an S5 layer-based world model, which predicts next world states in parallel during training and iteratively during environment interaction. Due to the special properties of S5 layers, our method can train in parallel and predict next world states iteratively during imagination. This allows for more efficient training than RNN-based world models and more efficient imagination than Transformer-based world models. We show that our approach outperforms the state of the art in terms of mean and median normalized human score on the Atari 100k benchmark, and that our proposed world model is able to predict complex dynamics very accurately. We also show that HIEROS displays superior exploration capabilities compared to existing approaches.

1. Introduction

Learning behavior from raw sensory input is a challenging task. Reinforcement learning (RL) is a field of machine learning that aims to solve this problem by learning a policy that maximizes the expected cumulative reward in an envi-

ronment (Sutton & Barto, 2018). The agent interacts with the environment by taking actions and receiving observations and rewards. The goal of the agent is to learn a policy that maximizes the expected cumulative reward. The agent can learn this policy by interacting with the environment and observing rewards, which is called model-free RL. Some agents also learn a model of their environment and learn a policy based on simulated environment states. This is called model-based RL (Moerland et al., 2023).

However, a significant hurdle encountered by RL algorithms is the lack of sample efficiency (Micheli et al., 2023). The demand for extensive interactions with the environment to learn an effective policy can be prohibitive in many real-world applications (Yampolskiy, 2018). In response to this challenge, deep reinforcement learning (DRL) has emerged as a promising solution. DRL leverages neural networks to represent and approximate complex policies and value functions, allowing it to tackle a wide array of problems and environments effectively.

One such approach is the concept of “world models”. World models aim to create a simulated environment within which the agent can generate an infinite amount of training data, thereby reducing the need for extensive interactions with the real environment (Ha & Schmidhuber, 2018). However, a key prerequisite for world models is the construction of precise models of the environment, a topic that has garnered substantial research attention (Hafner et al., 2022b; 2020; Kaiser et al., 2019). The idea of learning models of the agent’s environment has been around for a long time (Nguyen & Widrow, 1990; Schmidhuber, 1990; Jordan & Rumelhart, 1992). After being popularized by Ha & Schmidhuber (2018), world models have since evolved and diversified to address the sample efficiency problem more effectively. Most prominently, the DreamerV1-3 models (Hafner et al., 2020; 2022c; 2023) have achieved state-of-the-art results in multiple benchmarks such as Atari100k (Bellemare et al., 2013) or Minecraft (Kanitscheider et al., 2021). These models use a recurrent state space model (RSSM) (Hafner et al., 2022b) to learn a latent representation of the environment. The agent then uses this latent representation to train in imagination. Recently, Transformers have gained popularity as backbones for world models, due to their ability to capture complex dependencies in data. We

¹Anonymous Institution, Anonymous City, Anonymous Region, Anonymous Country. Correspondence to: Anonymous Author <anon.email@domain.com>.

Preliminary work. Under review by the International Conference on Machine Learning (ICML). Do not distribute.

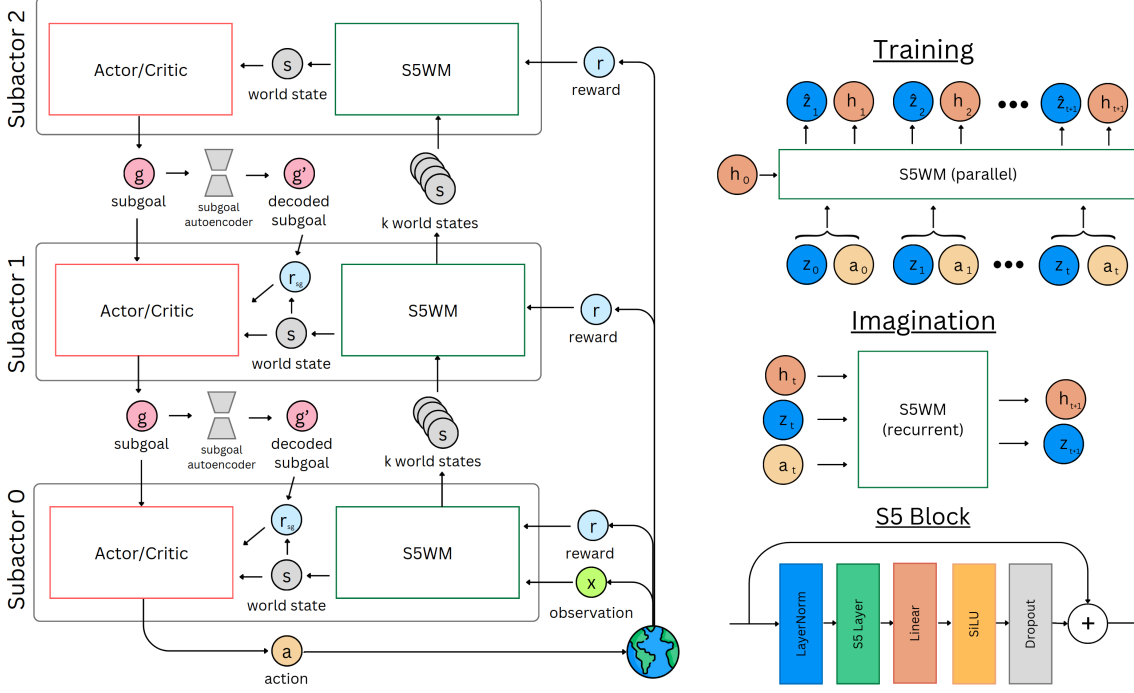


Figure 1. On the left: Hierarchical subactor structure of HIEROS. Each layer of the hierarchy learns its own latent state world model and interacts with the other layers via subgoal proposal. The action outputs of each actor/critic is the subgoal input of the next lower layer. The output of the lowest level actor/critic is the actual action in the real environment. On the right: Training and imagination procedure of the S5WM. HIEROS uses a stack of S5 blocks with their architecture shown above.

will discuss some approaches using Transformer-based architectures in Appendix B. One of the major drawbacks of those architectures is the inherent lack of runtime efficiency of the attention mechanism used in Transformers. Recently proposed structured state space sequence (S4) models (Gu et al., 2022) show comparable or superior performance in a wide range of tasks while being more runtime efficient than Transformer-based models, which makes them a promising alternative (Deng et al., 2023; Lu et al., 2023).

Another avenue for improving RL sample efficiency is hierarchical RL (HRL) (Dayan & Hinton, 1992; Parr & Russell, 1997; Sutton et al., 1999). This approach operates at different time scales, allowing the agent to learn and make decisions across multiple levels of abstraction. The idea is that higher level policies divide the environment task into smaller subtasks or subgoals (also commonly called skills). The lower level policy is then rewarded for fulfilling these subgoals and is thus guided to fulfill the overall environment task. This approach has been shown to be effective in a variety of tasks (Hafner et al., 2022a; Nachum et al., 2018; Jiang et al., 2019; Nachum et al., 2019a). Hafner et al. (2022a) proposes an HRL approach that builds on DreamerV2 (Hafner et al., 2022c) and achieves superior results in the Atari100k benchmark.

Finding the right experience replay buffer sampling strategy is key for many RL algorithms, as it has a great influence on

the final performance of the agent (Fedus et al., 2020; D’Oro et al., 2023). Li et al. (2023) introduce a time balanced replay dataset which empirically boosted the performance of their imagination based RL agent. However, this replay procedure relies on recomputing all probabilities in $O(n)$ at each iteration, which reduces its applicability for other approaches.

LeCun (2022) theorizes that an HRL agent that learns a hierarchy of world models and features intrinsic motivation to guide exploration could potentially achieve human-level performance in a wide range of tasks. Nachum et al. (2019c) and Aubret et al. (2023) provide further reasoning that combining HRL with other successful approaches such as world models could lead to a significant improvement in sample efficiency. Motivated by these findings, we propose HIEROS, a multilevel HRL agent that learns a hierarchy of world models, which use S5 layers to predict next world states. Specifically, our contributions are as follows:

- We introduce HIEROS, a Hierarchical Reinforcement Learning (HRL) agent designed to learn a hierarchy of world models, facilitating the acquisition of complex and temporally abstract behaviors. This enables HIEROS to project future environment states both far into the future and accurately for near-term interactions. Notably, our architecture is the first of its kind to employ hierarchical imagination within a multilevel

- framework, characterized by more than two layers.
- Furthermore, we propose S5WM, a world model architecture that leverages S5 layers to forecast subsequent world states. This model exhibits several advantageous properties compared to the RSSM used in DreamerV3 (Hafner et al., 2023) and several proposed Transformer-based alternatives (Micheli et al., 2023; Robine et al., 2023; Chen et al., 2022) as well as a recently proposed S4WM (Deng et al., 2023). Our novel contribution lies in leveraging the efficient design of our S5WM, capitalizing on its accessibility to the internal state, to effectively model environment dynamics in the context of imagination-based reinforcement learning.
 - We derive efficient time-balanced sampling (ETBS) for experience dataset sampling from the time-balanced sampling method proposed by Robine et al. (2023) with a sampling time complexity of $O(1)$.
 - We show that HIEROS achieves a new state-of-the-art mean and median normalized human score in the Atari100k benchmark (Bellemare et al., 2013).
 - We conduct a thorough ablation study that combining hierarchical imagination based learning and our S5WM yields superior results. We also test the impact of different design choices of HIEROS (e.g., world model choice, hierarchy depth, sampling procedure).

We describe our method in detail in Section 2. In Section 3, we evaluate HIEROS on the Atari100k benchmark (Bellemare et al., 2013) and analyze our results. Concluding remarks and ideas for future work are given in the final Section 4. We provide a section explaining some background concepts of the topic in Appendix A. In this introduction we already discussed several related works, however, we provide further comparisons with existing papers in Appendix B. In Appendix G we provide a wide range of ablation studies.

2. Methodology

In the context of RL, an agent interacts with an environment at discrete time steps, denoted as t . For the Atari 100K benchmark, for instance, where the environment represents a game like Pong, the agent’s interaction involves selecting an action a at time t within the game, similar to making in-game moves or pressing buttons. Subsequently, the agent receives an observation o and a reward r from the environment. In the case of Pong, o typically takes the form of a pixel image capturing the game’s visual state, while r represents the points earned as a result of the agent’s actions. The agent’s primary goal is to learn an optimal policy π , guiding its interactions with the environment, with the overarching objective of maximizing the expected cumulative reward, expressed as $\mathbb{E}[\sum_{t=0}^{\infty} \gamma^t r_t]$, where $\gamma < 1$ represents the discount factor and r_t stands for the reward at time step t .

In this section we introduce HIERarchical imagination On Structured state space sequence world models (HIEROS), a hierarchical model-based RL agent, that learns on trajectories generated by a Simplified Structured State Space Sequence (S5) model (Smith et al., 2023). We mainly base our approach upon DreamerV3 (Hafner et al., 2023) and Director (Hafner et al., 2022a). In the following section, we propose two major changes to the DreamerV3 architecture. First, we describe a hierarchical policy, where each abstraction layer learns its own S5 world model and an actor-critic. Second, we replace the world model with a world model based on S5 layers. We also introduce efficient time-based sampling (ETBS) method for true uniform sampling over the experience dataset with $O(1)$ time complexity.

2.1. Multilayered Hierarchical Imagination

HIEROS employs a goal conditioned hierarchical policy. Each abstraction layer learns its own S5 world model, an actor-critic and a subgoal autoencoder. We give some background on hierarchical reinforcement learning in Appendix A.2. The overall design of the subgoal proposal and the intrinsic reward computation is similar to the Director architecture (Hafner et al., 2022b), which successfully implements a hierarchical policy on the basis of DreamerV2. In contrast to Director and many other works, our architecture can easily be scaled to multiple hierarchy levels. Most approaches apply only one lower level and one higher level policy (Hafner et al., 2022a; Nachum et al., 2018; Jiang et al., 2019; Nair & Finn, 2019).

In Figure 1, we illustrate the hierarchical structure and interaction among subactors. Each subactor i comprises three modules: the world model (w_θ^i), an actor-critic component (π_ϕ^i), and a subgoal autoencoder (g_ψ^i). The world model imagines trajectories for the actor-critic training. The subgoal autoencoder compresses and decompresses states within the world model, with the decoder handling subgoal decoding, computing subgoal rewards r_g , and generating novelty rewards r_{nov} . Only the lowest layer (subactor 0) interacts directly with the environment. The higher layers receive k consecutive world model states from the lower level as observations, train their world model on these states and generate subgoals g_i . This is also in contrast to Director, which only provides the higher level policy with every k -th world state. We show the effect of providing all intermediate states as input for the higher level policy in Appendix G.5.

The subgoals represent world states that the lower layer is tasked to achieve. They are kept constant for k steps of the lower layer. So higher level subactors can only update their proposed subgoal every k steps of the next lower level. The actor-critic component is trained on imagined rollouts of the word model. The reward r is a mixture of extrinsic rewards r_{extr} (i.e. observed rewards directly from the environment),

165 subgoal rewards r_g , and novelty rewards r_{nov} :

$$r = r_{extr} + w_g \cdot r_g + w_{nov} \cdot r_{nov} \quad (1)$$

166 Here, w_g and w_{nov} are hyperparameters that control the
 167 influence of the subgoal and novelty rewards on the overall
 168 reward. The subgoal and novelty rewards r_g and r_{nov} are
 169 computed as follows:

$$r_{nov} = \|h_t - g_\psi^i(h_t)\|_2, \quad r_g = \frac{g_t^T \cdot h_t}{\max(\|g_t\|, \|h_t\|)} \quad (2)$$

170 with h_t being the deterministic world model state, g_ψ^i the
 171 subgoal autoencoder of subactor i , g_t the subgoal and $\|\cdot\|_2$
 172 being the L2 norm. Since the subgoal autoencoder is trained
 173 to compress and decompress the world model state, it is able
 174 to model the distribution of the observed model states. This
 175 allows using its reconstruction error on the current world
 176 model state as a novelty reward r_{nov} . The subgoal reward is
 177 computed using the cosine max similarity method between
 178 the world model state and the decompressed subgoal, which
 179 was proposed by (Hafner et al., 2022a).

180 The actor learns the policy:

$$a_t \sim \pi_\phi^i((h_t, z_t), g_t, r_t, c_t, H(p_\theta(z_t|m_t))) \quad (3)$$

181 with h_t and z_t representing the current model state, g_t being
 182 the subgoal, r_t being the reward, c_t being the continue
 183 signal, and $H(p_\theta(z_t|m_t))$ being the entropy of the latent
 184 state distribution. The entropy term is used to encourage
 185 exploration and make the actor aware of states with high
 186 uncertainty. These additional inputs to the actor network are
 187 motivated by findings of Robine et al. (2023) which show,
 188 that providing the predicted reward as input improves the
 189 learned policy. The actor is trained using the REINFORCE
 190 algorithm (Williams, 1992). In the case of a higher level
 191 subactor, a_t is the subgoal g_t for the next lower layer. The
 192 actor-critic trains three separate value networks for each
 193 reward term to predict their future mean return. The subgoal
 194 autoencoder g_ψ^i is composed of an encoder and a decoder:

$$\text{Encoder: } g_t \sim p_\psi(g_t|h_t), \quad \text{Decoder: } h_t \approx f_\psi(g_t) \quad (4)$$

195 The deterministic part h_t of the model state is the only input
 196 for the subgoal autoencoder. This choice is made because
 197 the stochastic part z_t is less controllable by the lower-level
 198 actor, making the subgoal less achievable. Hafner et al.
 199 (2022a) found that the full latent state space of the lower
 200 level world model as action space would constitute a high
 201 dimensional continuous control problem for the higher level
 202 actor, which is hard for a policy to optimize on. Instead, the
 203 g_ψ^i compresses the latent state into a discrete subgoal space
 204 of 8 categorical vectors of size 8. This compressed action
 205 space is much easier to navigate for the subgoal proposing
 206 policy than the continuous world state. While Hafner
 207 et al. (2022a) uses the decompressed goal as input for their
 208 worker policy, our approach with HIEROS demonstrates
 209 improved subgoal completion and overall higher rewards
 210 when training subactors on the compressed subgoals. We
 211 directly compare these two approaches in Appendix G.7.
 212 The subgoal autoencoder is trained using a variational loss:

213 $\mathcal{L}_\psi = \|f_\psi(z) - h_t\|_2 + \beta \cdot KL[p_\psi(g_t|h_t) || q(g_t)]$
 214 (5)

215 z is sampled from the encoder distribution $z \sim p_\psi(g_t|h_t)$
 216 and $q(g_t)$ is a uniform prior. β is a hyperparameter controlling
 217 the impact of KL divergence on the overall loss. All experiment
 218 hyperparameters are listed in Appendix E. Following DreamerV3
 219 (Hafner et al., 2023), Hieros' hyperparameters remain fixed unless
 220 otherwise specified (e.g., in ablation experiments).

221 Subgoals from all hierarchy layers can be decoded into the
 222 game's original image space, enabling visualization of the
 223 agent's objectives and making HIEROS actions explainable.
 224 Examples are presented in Appendix D.

2.2. S5-based World Model (S5WM)

225 The world model in HIEROS is responsible for imagining
 226 a trajectory of future world states. For this task, we use
 227 a similar architecture as DreamerV3 while swapping out
 228 the RNN-based sequence model for an S5-based sequence
 229 model. We give some background on world models and
 230 S4/S5 layers in Appendices A.1 and A.3. Our world model
 231 consists of the networks:

$$\begin{aligned} \text{Sequence model: } & (m_t, h_t) = f_\theta(h_{t-1}, z_{t-1}, a_{t-1}) \\ \text{Encoder: } & z_t \sim q_\theta(z_t | o_t) \\ \text{Dynamics predictor: } & \hat{z}_t \sim p_\theta(\hat{z}_t | m_t) \\ \text{Reward predictor: } & \hat{r}_t \sim p_\theta(\hat{r}_t | h_t, z_t) \\ \text{Continue predictor: } & \hat{c}_t \sim p_\theta(\hat{c}_t | h_t, z_t) \\ \text{Decoder: } & \hat{o}_t \sim p_\theta(\hat{o}_t | h_t, z_t) \end{aligned}$$

232 With o_t being the observation at time step t , m_t the output of
 233 the sequence model, and h_t the internal state of the S5 layers
 234 in the sequence model, which we use as the deterministic
 235 part of the world state. z_t is the stochastic part of the latent
 236 world state, a_t the action taken, \hat{z}_t the predicted latent state,
 237 \hat{r}_t the predicted extrinsic reward, \hat{c}_t the predicted continue
 238 signal and \hat{o}_t the decoded observation. Figure 1 shows the
 239 overall structure of the world model.

240 During training, S5WM processes sequential observations
 241 $o_0 \dots o_t$ and actions $a_0 \dots a_{t-1}$. The encoder computes
 242 posterior z_t from o_t , while the sequence model predicts
 243 output m_t and deterministic state h_t . Using h_t alongside m_t
 244 in predicting dynamics would be possible but doesn't add
 245 extra information. The posterior z_t represents the stochastic

state with knowledge of the actual observation o_t , while the prior \hat{z}_t is the stochastic state predicted solely from the deterministic sequence model output. During imagination, the actor only has access to the prior \hat{z} .

The RSSM encoder in DreamerV3 computes the posterior from both o_t and the deterministic model state h_t , which makes the parallel computation of z_t impossible. However, Chen et al. (2022) show, that accurate representation can also be learned by making the posterior z_t independent of h_t and only predict the distribution $p(z_t|o_t)$.

As detailed in Appendix A.3, S5 and S4 layers allow for both parallel sequence modeling and iterative autoregressive next state prediction. This makes them more efficient than RNNs for model training and more efficient than Transformer-based models for imagination. While Deng et al. (2023) propose S4WM, an S4-based world model, our use of S5 layers is advantageous. S5 layers excel in modeling longer-term dependencies and are more memory-efficient. Moreover, the direct accessibility of the latent state x_t in S5 layers enables HIEROS to utilize the recurrent model state as the deterministic component of the world state h_t . This contrasts with other approaches that rely on using the sequence model output as deterministic world model states (Chen et al., 2022; Deng et al., 2023; Micheli et al., 2023), which proves less effective in our experiments (Appendix G.2).

We use a modified version of an S5 layer, which was proposed by Lu et al. (2023). They introduce a reset mechanism, which allows setting the internal state h_t to its initial value h_0 during the parallel sequence prediction by also passing the continue signal $c_0 \dots c_n$ to the sequence model. This allows the actor to train on trajectories that span multiple episodes without leaking information from the end of one episode to the beginning of the next. We employ the same mechanism for our S5WM, as trajectories spanning episode borders are commonly encountered during training. It is unclear if the S4WM proposed in Deng et al. (2023) faced the same challenge and if and how they solved it.

The sequence model of our S5WM uses a stack of multiple S5 blocks, as depicted in Figure 1. The design of this block is inspired by the deep sequence model architecture proposed by Smith et al. (2023) but we selected a different norm layer, dropout and activation function. The number of blocks used is listed in Appendix E. All parts of S5WM are optimized jointly using a loss function that follows the loss function of DreamerV3:

$$\mathcal{L}(\theta) = \mathcal{L}_{pred}(\theta) + \alpha_{dyn} \cdot \mathcal{L}_{dyn}(\theta) + \alpha_{rep} \cdot \mathcal{L}_{rep}(\theta) \quad (6)$$

$$\begin{aligned} \mathcal{L}_{pred}(\theta) &= -\ln(p_\theta(r_t|h_t, z_t)) - \ln(p_\theta(c_t|h_t, z_t)) \\ &\quad - \ln(p_\theta(o_t|h_t, z_t)) \end{aligned} \quad (7)$$

$$\mathcal{L}_{dyn}(\theta) = \max(1, \text{KL}[\text{sg}(q_\theta(z_t|o_t)) || p_\theta(z_t|m_t)]) \quad (8)$$

$$\mathcal{L}_{rep}(\theta) = \max(1, \text{KL}[q_\theta(z_t|o_t) || \text{sg}(p_\theta(z_t|m_t))]) \quad (9)$$

For \mathcal{L}_{dyn} and \mathcal{L}_{rep} we use the method of free bits introduced by Kingma et al. (2016) and used in DreamerV3 (Hafner et al., 2023) to prevent the dynamics and representations from collapsing into easily predictable distributions. α_{dyn} and α_{rep} are hyperparameters that control the influence of the dynamics and representation loss.

2.3. Efficient Time-balanced Sampling

When interacting with the environment, HIEROS collects observations, actions, and rewards in an experience dataset. After a fixed number of interactions, trajectories are sampled from the dataset in order to train the world model, actor, and subgoal autoencoder. DreamerV3 (Hafner et al., 2023) uses a uniform sampling. This, however, leads to an oversampling of the older entries of the dataset, as the iterative uniform sampling can select these entries more often than newer ones. As explained in Section 1 Robine et al. (2023) solve this using a time-balanced replay buffer with a $O(n)$ sampling runtime complexity with n being the size of the replay buffer.

We propose an efficient time-balanced sampling method (ETBS), which produces similar results with $O(1)$ time complexity. When iteratively adding elements to the experience replay dataset and afterward sampling uniformly, the expected number of times N_{x_i} an element x_i has been drawn after n iterations is

$$\mathbb{E}(N_{x_i}) = \frac{1}{i} + \frac{1}{i+1} + \dots + \frac{1}{n} = H_n - H_i \quad (10)$$

with H_i being the i -th harmonic number. The probability of sampling x_i , $i = 1, \dots, n$, is

$$p_i = \frac{1}{n} \cdot \mathbb{E}(N_{x_i}) = \frac{H_n - H_i}{n} \approx \frac{\ln(n) - \ln(i)}{n} \quad (11)$$

We use the approximation $H_x \approx \ln(x)$ to remove the need to compute harmonic values. The idea is, to compute the CDF of this probability distribution between 0 and n to transform samples from the imbalanced distribution into uniform samples via probability integral transformation (David & Johnson, 1948). How we derive the CDF of this distribution is shown in Appendix H. With the CDF we compute the ETBS probabilities as follows:

$$p_{etbs}(x) = CDF(p(x)) \cdot \tau + p(x) \cdot (1 - \tau) \quad (12)$$

with p being the original sampling distribution, CDF being the CDF of the original distribution and τ being a temperature hyperparameter that controls the influence of the original distribution on the overall distribution. We set τ to 0.3 in our experiments. Empirically, a slight oversampling of earlier experiences seems to have a positive influence on the actor performance. The time complexity of this sampling method is $O(1)$, as the CDF can be precomputed and the sampling is done in constant time. For further details, see Appendix H.

Task	Mean	Median	IQM	Optimality Gap
Random	0	0	0	100
Human	100	100	100	0
SimPLE	34	11	13	73
TWM	96	50	46	52
IRIS	105	29	50	51
DreamerV3	112	49	N/A	N/A
Hieros (ours)	120	56	53	49

Table 1. Aggregate scores of HIEROS and baselines on the Atari100k test suite. Higher scores for Mean, Median and IQM are better. For Optimality Gap, lower scores are better. DreamerV3 does not report the scores for IQM or Optimality Gap. We show the best results for each row in **bold** font.

3. Experiments

We evaluate the performance of HIEROS on the Atari100k test suite (Bellemare et al., 2013), which contains a wide range of games with different dynamics and objectives. In each of these environments, the agent is only allowed 100k interaction with the environment, which amounts to roughly 2 hours of total gameplay. We evaluate HIEROS on a subset of 25 of those games. We compare HIEROS to the following baselines: DreamerV3 (Hafner et al., 2023), IRIS (Micheli et al., 2023), TWM (Robine et al., 2023), and SimpPLE (Kaiser et al., 2019). SimPLE trains a policy on the direct pixel input of the environment using PPO (Schulman et al., 2017), while TWM, IRIS and DreamerV3 train a policy on imagined trajectories of a world model. TWM and IRIS use a Transformer-based world model. IRIS, however, trains the agent not in the latent space of the world model but in the decoded state space of the environment, which is one of the main differences to other approaches that leverage a Transformer-based world model (e.g. TWM). Ye et al. (2021) propose EfficientZero, which holds the current absolute state of the art in the Atari100k test suite. However, this method relies on look-ahead search during policy inference and is thus not comparable to the other methods.

Comparing our S5WM against the S4WM proposed by Deng et al. (2023) would be interesting, as both models are based on structured state spaces. However, Deng et al. (2023) only report results on their proposed set of memory testing environments and their code base is not public yet. So we are not able to compare our results directly to theirs. We do however compare our S5WM to the RSSM used in DreamerV3 in Section 3.2. The used computation resources, implementation details and a link to the source code can be found in Appendix F. We use the hyperparameters as specified in Appendix E for all experiments.

3.1. Results for the Atari100k Test Suite

All scores are the average of three runs with different seeds. To aggregate the results, we compute the normalized human score (Bellemare et al., 2013), which is defined as $(score_{agent} - score_{random}) / (score_{human} - score_{random})$. We show the achieved aggregated mean and median normalized human score in Table 1. The full table with scores for all games can be found in Appendix C.

Our model achieves a new state of the art in regard to the mean and median normalized human score. We also achieve a new state of the art in regard to the achieved reward on 9 of the 25 games. Adhering to Agarwal et al. (2021), we also report the optimality gap and the interquartile mean (IQM) of the human normalized scores and achieve state-of-the-art results in both of those metrics. HIEROS outperforms the other approaches while having significant advantages with regard to runtime efficiency during training and inference, as well as resource demand. For training on a single Atari game for 100k steps, TWM takes roughly 0.8 days on a A100 GPU, while DreamerV3 takes 0.5 days and IRIS takes 7 days. Hieros takes roughly 14 hours \approx 0.6 days and is thus significantly faster than IRIS while being on par with DreamerV3 and TWM.

Significant improvements were achieved in Frostbite, James-Bond, and PrivateEye. These games feature multiple levels with changing dynamics and reward distributions. In order for the S5WM to learn to simulate these levels, the actor needs to employ a sufficient exploration strategy to discover these levels. This shift in the state distribution poses a challenge for many imagination-based approaches (Micheli et al., 2023). HIEROS is able to overcome this challenge by using the proposed subgoals on different time scales to guide the agent towards the next level. We show in Appendix D different proposed subgoals which guide the lower level actor to finding the way to the next level by building the igloo in the upper right part of the image.

HIEROS seems to perform significantly worse than other approaches in Breakout or Pong, which feature no significant shift in states or dynamics. It seems as if the hierarchical structure makes it harder to grasp the relatively simple dynamics of these games, as the dynamics remain the same across all time abstractions. This is backed by our findings in Appendix G.3 that HIEROS with only one subactor performs significantly better on Breakout. We also show empirically in Section 3.2 that using the S5WM also seems to deteriorate the performance of HIEROS in those games compared to the RSSM used for DreamerV3. Figure 5 shows some proposed subgoals for Breakout. The subgoals seem only to propose to increase the level score, which is does not provide the lower level agent any indication on how to do so. So the lower level actor is not able to benefit from the hierarchical structure in these games.

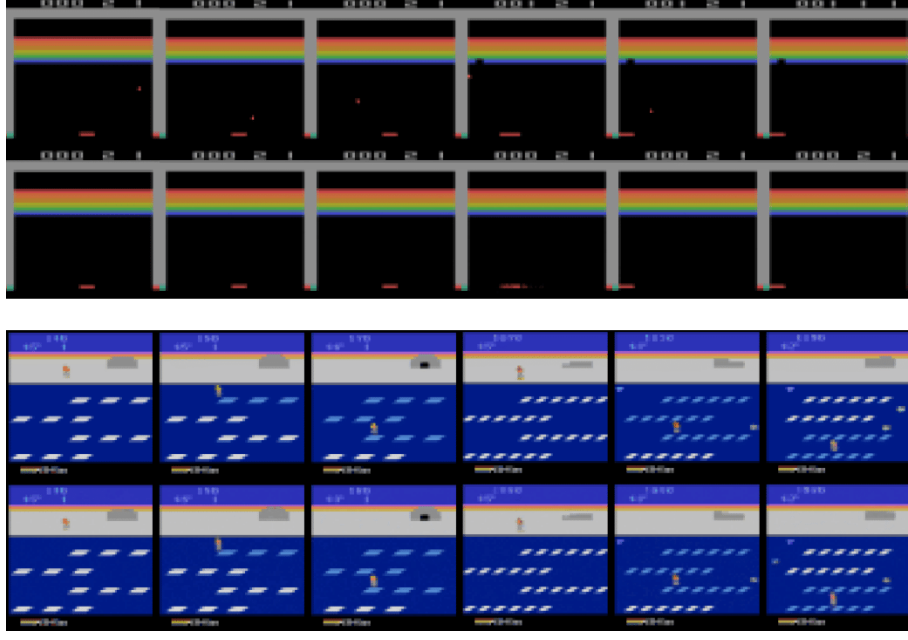


Figure 2. Trajectories for Breakout (top) and Frostbite (bottom). For each, the upper frame is the image observed in the environment and the lower frames are the imagined trajectories of the S5WM of the lowest level subactor.

Figure 3 shows the partial rewards r_{extr} , r_{nov} , and r_{sg} for the lowest level subactor for Breakout and Krull, another game featuring multiple levels similar to Frostbite. As can be seen, the extrinsic rewards for Breakout are very sparse and do not provide any indication on how to increase the level score. So the subactor learns to follow the subgoals from the higher levels more closely instead, which in the case of Breakout or Pong does not lead to a better performance. In Krull however, the extrinsic rewards are more frequent and provide a better indication on how to increase the level score. So the subactor is able to learn to follow the subgoals from the higher levels more loosely, treating them more like a hint, and is able to achieve a better performance.

3.2. Imagined Trajectories

In Figure 2, we show an observed trajectory for the games Frostbite and Breakout alongside the imagined trajectories of the S5WM of the lowest level subactor. As can be seen, the world model is not able to predict the movement of the ball in breakout. This indicates that the model is not able to model the very small impact of the ball movement to the change in the image. We found that during random exploration at the beginning of the training the events where the ball bounces back from the moving plateau are very rare and most of the time the ball is lost before it can bounce back. This makes it difficult for the world model to learn the dynamics of the ball movement and their impact on the reward distribution. We make similar observations for the game Pong.

S4-based models are shown to perform worse than Transformer models on short term sequence modeling tasks (Zuo et al., 2022; Mehta et al., 2022; Dao et al., 2022) while excelling on long term modeling tasks. This could also give some reasoning why our S5WM seems to perform worse on Breakout or Pong compared to Frostbite or Krull. Freeway poses a similar challenge, with sparse rewards that are only achieved after a complex series of environment interaction. However, unlike with Breakout and Pong, in Freeway HIEROS is able to profit from its hierarchical structure in order to guide exploration. An example of this can be seen in Figure 5, where the subgoals are able to guide the agent across the road. S5WM is able to accurately capture the multiple levels of Frostbite, despite only having access to train on these levels after discovering them, which usually happens after roughly 50k interactions. As the reaching of the next level is directly connected to a large increase in rewards, the S5WM is able to correctly predict the next level after only a few interactions. This is also reflected in the significantly higher reward achieved by HIEROS.

To directly compare the influence of our S5WM architecture to the RSSM used in DreamerV3, we replace the S5WM with an RSSM and train HIEROS on four different games. The results are shown in Appendix G.1. The RSSM is not able to achieve the same performance as the S5WM for Krull, Battle Zone and Freeway, but is slightly better compared to using the S5WM for Breakout. In Figure 4 we show the world model losses for S5WM and RSSM for Krull and Breakout. The S5WM consistently achieves lower overall loss than the RSSM in Krull, whereas this trend reverses

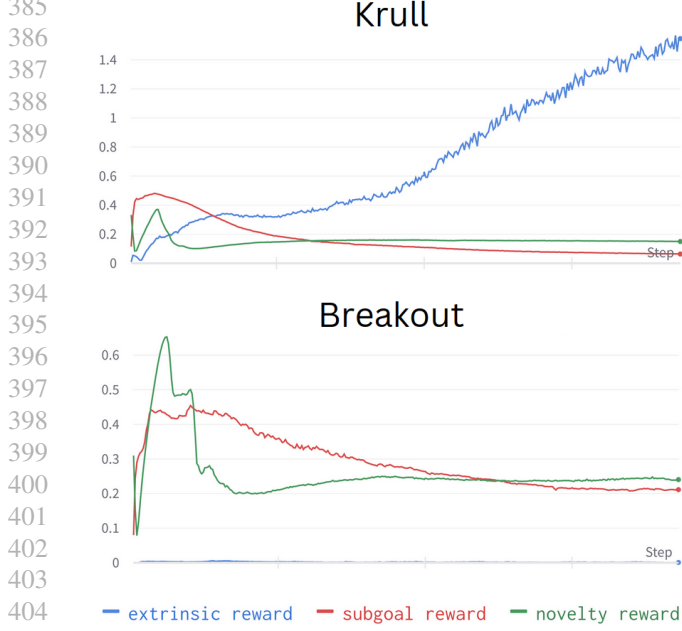


Figure 3. Extrinsic, subgoal, and novelty rewards per step for Krull (top) and Breakout (bottom) for the lowest level subactor.

for Breakout. Given the substantially higher absolute loss values for the more complex Krull compared to Breakout, we infer that the larger S5WM excels in environments with complex dynamics and substantial input distribution shifts. In contrast, the smaller RSSM is better suited for environments with simple dynamics and a stable input distribution.

As both models are trained with the same number of gradient updates, it makes sense that the larger model has difficulties matching the performance of the smaller model in non-shifting environments with simple dynamics. So a smaller S5WM might achieve better results for Breakout. We test this hypothesis in Appendix G.6. Lu et al. (2023) and Deng et al. (2023) find that structured state space models generally surpass RNNs in terms of memory recollection and resilience to distribution shifts, which we can confirm with our results. Moreover, we perform further ablations in Appendix G.

4. Conclusion

In this paper, we introduce the HIEROS architecture, a multilayered goal conditioned hierarchical reinforcement learning (HRL) algorithm with hierarchical world models, an S5 layer-based world model (S5WM) and an efficient time-balanced sampling (ETBS) method which allows for a true uniform sampling over the experience dataset. We evaluate HIEROS on the Atari100k test suite (Bellemare et al., 2013) and achieve a new state of the art mean human normalized score for model-based RL agents without look-ahead search.

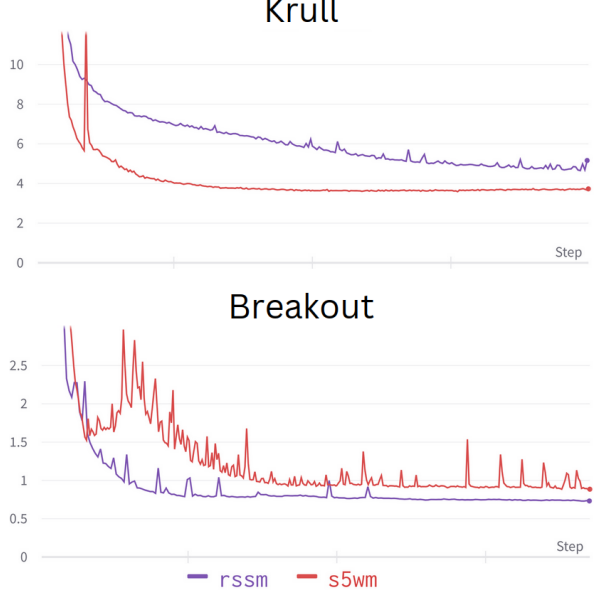


Figure 4. World model losses for the S5WM and RSSM for Krull and Breakout. The S5WM is able to achieve an overall lower world model loss compared to the RSSM for Krull, while those roles are reversed for Breakout.

The option to decode proposed subgoals gives some explainability to the actions taken by HIEROS. A deeper evaluation on which subgoals are proposed and how the lower level workers are able to achieve these subgoals is left for future research. The S5WM poses multiple improvements compared to RNN-based world models (Hafner et al., 2023) (i.e. efficiency during training, prediction accuracy during imagination) and Transformer-based world models (Chen et al., 2022; Robine et al., 2023; Micheli et al., 2023) (i.e. prediction accuracy and efficiency during imagination). A thorough comparison between our S5WM and the S4WM proposed by Deng et al. (2023) remains for future research. We delve deeper into further directions for future research in Appendix I.

For now, we only evaluated Hieros on the Atari100k benchmark (Ye et al., 2021), but experiments on further benchmarks are necessary. BSuite (Osband et al., 2020) is a collection of low dimensional experiments directed at creating a detailed profile of an RL algorithm in several categories, e.g. long term memory, exploration or robustness against stochasticity. The Deep Mind Control Suite (Tassa et al., 2018) contains several continuous control tasks for robots in different sizes and shapes. Also, Crafter (Hafner, 2021), a complex 2D environment with difficult exploration tasks, would give deeper insights in how Hieros' exploration capabilities compare with other state-of-the-art approaches. For now, we leave these further evaluations to future work.

With our work, we hope to provide a new perspective on the field of HRL and to inspire future research in this field.

440 Reproducibility Statement

441
442 We describe all important architectural and training de-
443 tails in Section 2 and provide the used hyperparam-
444 eters in Appendix E. We provide the source code
445 in the supplementary material and under the follow-
446 ing link: <https://anonymous.4open.science/r/Hieros-7C37/>. The material also gives an expla-
447 nition on how to install and use the Atari100k benchmark for
448 reproducing our results. The computational resources we
449 used for our experiments are described in Appendix F.
450

451 Impact Statement

452 Autonomous agents pose many ethical concerns, as they are
453 able to act in the real world and can cause harm to humans.
454 In our work, we only use simulated environments and do
455 not see any potential for misuse of our work. We propose a
456 new world model architecture which could be used to train
457 agents in imagination rather than in the real world. This
458 could be used to train agents for real-world applications,
459 such as autonomous driving, without the need to train them
460 in the real world. This could reduce the risk of harm to
461 humans and the environment.

464 References

- 466 Agarwal, P., Andrews, S., and Kahou, S. E. Learning to
467 play atari in a world of tokens. 2023.
- 468 Agarwal, R., Schwarzer, M., Castro, P. S., Courville, A. C.,
469 and Bellemare, M. Deep reinforcement learning at the
470 edge of the statistical precipice. *Advances in Neural*
471 *Information Processing Systems*, 34:29304–29320, 2021.
- 472 Aubret, A., Matignon, L., and Hassas, S. An information-
473 theoretic perspective on intrinsic motivation in reinforce-
474 ment learning: A survey. *Entropy*, 25(2):327, 2023. ISSN
475 1099-4300. doi: 10.3390/e25020327. URL <https://www.mdpi.com/1099-4300/25/2/327>. Number:
476 2 Publisher: Multidisciplinary Digital Publishing
477 Institute.
- 478 Bellemare, M. G., Naddaf, Y., Veness, J., and Bowling, M.
479 The arcade learning environment: An evaluation plat-
480 form for general agents. *Journal of Artificial Intelligence*
481 *Research*, 47:253–279, 2013.
- 482 C2D. S5: Simplified state space layers for sequence model-
483 ing, 2023. URL <https://github.com/i404788/s5-pytorch>. original-date: 2023-03-20T23:57:07Z.
- 484 Chen, C., Wu, Y.-F., Yoon, J., and Ahn, S. TransDreamer:
485 Reinforcement learning with transformer world mod-
486 els, 2022. URL <https://arxiv.org/abs/2202.09481>. arXiv:2202.09481.
- 487 Cho, K., Van Merriënboer, B., Gulcehre, C., Bahdanau,
488 D., Bougares, F., Schwenk, H., and Bengio, Y. Learning
489 phrase representations using rnn encoder-decoder
490 for statistical machine translation. *arXiv preprint*
491 *arXiv:1406.1078*, 2014.
- 492 Dao, T., Fu, D. Y., Saab, K. K., Thomas, A. W., Rudra,
493 A., and Ré, C. Hungry hungry hippos: Towards lan-
494 guage modeling with state space models. *arXiv preprint*
495 *arXiv:2212.14052*, 2022.
- 496 David, F. and Johnson, N. The probability integral transfor-
497 mation when parameters are estimated from the sample.
498 *Biometrika*, 35(1/2):182–190, 1948.
- 499 Dayan, P. and Hinton, G. E. Feudal reinforcement learning.
500 *Advances in Neural Information Processing Systems*, 5,
501 1992.
- 502 Deng, F., Park, J., and Ahn, S. Facing off
503 world model backbones: RNNs, transformers, and
504 S4, 2023. URL <http://arxiv.org/abs/2307.02064>. arXiv:2307.02064.
- 505 D’Oro, P., Schwarzer, M., Nikishin, E., Bacon, P.-L., Bellemare, M. G., and Courville, A. Sample-efficient reinforcement learning by breaking the replay ratio barrier. In *The Eleventh International Conference on Learning Representations*, 2023. URL <https://openreview.net/forum?id=OpC-9aBBVJe>.
- 506 Fedus, W., Ramachandran, P., Agarwal, R., Bengio, Y., Larochelle, H., Rowland, M., and Dabney, W. Revisiting fundamentals of experience replay. In *International Conference on Machine Learning*, pp. 3061–3071. PMLR, 2020.
- 507 Florensa, C., Duan, Y., and Abbeel, P. Stochastic neural networks for hierarchical reinforcement learning. *arXiv preprint arXiv:1704.03012*, 2017.
- 508 Gu, A., Goel, K., and Ré, C. Efficiently modeling long sequences with structured state spaces, 2022. URL <http://arxiv.org/abs/2111.00396>. arXiv:2111.00396.
- 509 Gumbesch, C., Sajid, N., Martius, G., and Butz, M. V. Learning hierarchical world models with adaptive temporal abstractions from discrete latent dynamics. In *The Twelfth International Conference on Learning Representations*, 2023.
- 510 Gupta, A., Mehta, H., and Berant, J. Simplifying and under-
511 standing state space models with diagonal linear rnns.
512 *arXiv preprint arXiv:2212.00768*, 2022.
- 513 Ha, D. and Schmidhuber, J. World models. *arXiv preprint*
514 *arXiv:1803.10122*, 2018.

- 495 Hafner, D. Benchmarking the spectrum of agent capabilities.
 496 *arXiv preprint arXiv:2109.06780*, 2021.
- 497 Hafner, D., Lillicrap, T., Ba, J., and Norouzi, M. Dream
 498 to control: Learning behaviors by latent imagination,
 499 2020. URL <http://arxiv.org/abs/1912.01603>. arXiv:1912.01603.
- 500 Hafner, D., Lee, K.-H., Fischer, I., and Abbeel, P. Deep
 501 hierarchical planning from pixels, 2022a. URL <http://arxiv.org/abs/2206.04114>. arXiv:2206.04114.
- 502 Hafner, D., Lee, K.-H., Fischer, I., and Abbeel, P.
 503 Learning latent dynamics for planning from pixels.
 504 2022b. URL <http://arxiv.org/abs/2206.04114>. arXiv:2206.04114.
- 505 Hafner, D., Lillicrap, T., Norouzi, M., and Ba, J. Mastering
 506 atari with discrete world models, 2022c. URL <http://arxiv.org/abs/2010.02193>. arXiv:2010.02193.
- 507 Hafner, D., Pasukonis, J., Ba, J., and Lillicrap,
 508 T. Mastering diverse domains through world
 509 models, 2023. URL <http://arxiv.org/abs/2301.04104>. arXiv:2301.04104.
- 510 Hutsebaut-Buysse, M., Mets, K., and Latré, S. Hierar-
 511 chical reinforcement learning: A survey and open re-
 512 search challenges. *Machine Learning and Knowledge
 513 Extraction*, 4(1):172–221, 2022. ISSN 2504-4990. doi:
 514 10.3390/make4010009. URL <https://www.mdpi.com/2504-4990/4/1/9>. Number: 1 Publisher: Mu-
 515 ltidisciplinary Digital Publishing Institute.
- 516 Jiang, Y., Gu, S., Murphy, K., and Finn, C. Language as
 517 an abstraction for hierarchical deep reinforcement learn-
 518 ing, 2019. URL <http://arxiv.org/abs/1906.07343>. arXiv:1906.07343.
- 519 Jordan, M. I. and Rumelhart, D. E. Forward mod-
 520 els: Supervised learning with a distal teacher.
 521 *Cognitive Science*, 16(3):307–354, 1992. doi:
 522 https://doi.org/10.1207/s15516709cog1603_1. URL
 523 https://onlinelibrary.wiley.com/doi/abs/10.1207/s15516709cog1603_1.
- 524 Kaiser, L., Babaeizadeh, M., Milos, P., Osinski, B., Camp-
 525 bell, R. H., Czechowski, K., Erhan, D., Finn, C., Koza-
 526 kowski, P., Levine, S., et al. Model-based reinforce-
 527 ment learning for atari. *arXiv preprint arXiv:1903.00374*,
 528 2019.
- 529 Kanitscheider, I., Huizinga, J., Farhi, D., Guss, W. H.,
 530 Houghton, B., Sampedro, R., Zhokhov, P., Baker, B.,
 531 Ecoffet, A., Tang, J., et al. Multi-task curriculum learning
 532 in a complex, visual, hard-exploration domain: Minecraft.
 533 *arXiv preprint arXiv:2106.14876*, 2021.
- 534 Kingma, D. P., Salimans, T., Jozefowicz, R., Chen, X.,
 535 Sutskever, I., and Welling, M. Improved variational in-
 536 ference with inverse autoregressive flow. *Advances in
 537 Neural Information Processing Systems*, 29, 2016.
- 538 Koul, A., Kumar, V. V., Fern, A., and Majumdar, S. Dream
 539 and search to control: Latent space planning for continu-
 540 ous control. *arXiv preprint arXiv:2010.09832*, 2020.
- 541 Kujanpää, K., Pajarin, J., and Ilin, A. Hierar-
 542 chical imitation learning with vector quantized mod-
 543 els, 2023. URL <http://arxiv.org/abs/2301.12962>. arXiv:2301.12962.
- 544 LeCun, Y. A path towards autonomous machine intelligence
 545 version 0.9. 2, 2022-06-27. *Open Review*, 62, 2022.
- 546 Li, J., Tang, C., Tomizuka, M., and Zhan, W. Hierar-
 547 chical planning through goal-conditioned offline rein-
 548 forcement learning, 2022. URL <http://arxiv.org/abs/2205.11790>. arXiv:2205.11790.
- 549 Li, Y., Ildiz, M. E., Papailiopoulos, D., and Oymak, S.
 550 Transformers as algorithms: Generalization and stability
 551 in in-context learning, 2023. URL <http://arxiv.org/abs/2301.07067>. arXiv:2301.07067.
- 552 Lu, C., Schroecker, Y., Gu, A., Parisotto, E., Foer-
 553 ster, J., Singh, S., and Behbahani, F. Structured
 554 state space models for in-context reinforcement learn-
 555 ing, 2023. URL <http://arxiv.org/abs/2303.03982>. arXiv:2303.03982.
- 556 Mehta, H., Gupta, A., Cutkosky, A., and Neyshabur, B.
 557 Long range language modeling via gated state spaces.
 558 *arXiv preprint arXiv:2206.13947*, 2022.
- 559 Micheli, V., Alonso, E., and Fleuret, F. Transformers are
 560 sample-efficient world models, 2023. URL <http://arxiv.org/abs/2209.00588>. arXiv:2209.00588.
- 561 Moerland, T. M., Broekens, J., Plaat, A., Jonker, C. M.,
 562 et al. Model-based reinforcement learning: A survey.
 563 *Foundations and Trends® in Machine Learning*, 16(1):
 564 1–118, 2023.
- 565 Nachum, O., Gu, S., Lee, H., and Levine, S. Data-
 566 efficient hierarchical reinforcement learning, 2018.
 567 URL <http://arxiv.org/abs/1805.08296>. arXiv:1805.08296.
- 568 Nachum, O., Ahn, M., Ponte, H., Gu, S., and Kumar, V.
 569 Multi-agent manipulation via locomotion using hierar-
 570 chical Sim2Real, 2019a. URL <http://arxiv.org/abs/1908.05224>. arXiv:1908.05224.
- 571 Nachum, O., Gu, S., Lee, H., and Levine, S. Near-optimal
 572 representation learning for hierarchical reinforcement

- learning, 2019b. URL <http://arxiv.org/abs/1810.01257>. arXiv:1810.01257.
- Nachum, O., Tang, H., Lu, X., Gu, S., Lee, H., and Levine, S. Why does hierarchy (sometimes) work so well in reinforcement learning?, 2019c. URL <http://arxiv.org/abs/1909.10618>. arXiv:1909.10618.
- Nair, S. and Finn, C. Hierarchical foresight: Self-supervised learning of long-horizon tasks via visual subgoal generation, 2019. URL <http://arxiv.org/abs/1909.05829>. arXiv:1909.05829.
- Nguyen, D. and Widrow, B. The truck backer-upper: An example of self-learning in neural networks. In *Advanced neural computers*, pp. 11–19. Elsevier, 1990.
- NM512. dreamerv3-torch, 2023. URL <https://github.com/NM512/dreamerv3-torch>. original-date: 2023-02-11T23:23:26Z.
- Okada, M. and Taniguchi, T. Dreaming: Model-based reinforcement learning by latent imagination without reconstruction, 2021. URL <http://arxiv.org/abs/2007.14535>. arXiv:2007.14535.
- Osband, I., Doron, Y., Hessel, M., Aslanides, J., Sezener, E., Saraiva, A., McKinney, K., Lattimore, T., Szepesvári, C., Singh, S., Van Roy, B., Sutton, R., Silver, D., and van Hasselt, H. Behaviour suite for reinforcement learning. In *International Conference on Learning Representations*, 2020. URL <https://openreview.net/forum?id=rygf-kSYwH>.
- Parr, R. and Russell, S. Reinforcement learning with hierarchies of machines. *Advances in Neural Information Processing Systems*, 10, 1997.
- Poudel, R. P. K., Pandya, H., and Cipolla, R. Contrastive unsupervised learning of world model with invariant causal features, 2022. URL <http://arxiv.org/abs/2209.14932>. arXiv:2209.14932.
- Robine, J., Höftmann, M., Uelwer, T., and Harmeling, S. Transformer-based world models are happy with 100k interactions, 2023. URL <http://arxiv.org/abs/2303.07109>. arXiv:2303.07109.
- Rosete-Beas, E., Mees, O., Kalweit, G., Boedecker, J., and Burgard, W. Latent plans for task-agnostic offline reinforcement learning. In *Conference on Robot Learning*, pp. 1838–1849. PMLR, 2023.
- Schmidhuber, J. An on-line algorithm for dynamic reinforcement learning and planning in reactive environments. In *1990 IJCNN international joint conference on neural networks*, pp. 253–258. IEEE, 1990.
- Schulman, J., Wolski, F., Dhariwal, P., Radford, A., and Klimov, O. Proximal policy optimization algorithms. *arXiv preprint arXiv:1707.06347*, 2017.
- Schwarzer, M., Rajkumar, N., Noukhovitch, M., Anand, A., Charlin, L., Hjelm, D., Bachman, P., and Courville, A. Pretraining representations for data-efficient reinforcement learning, 2021. URL <http://arxiv.org/abs/2106.04799>. arXiv:2106.04799.
- Smith, J. T. H., Warrington, A., and Linderman, S. W. Simplified state space layers for sequence modeling, 2023. URL <http://arxiv.org/abs/2208.04933>. arXiv:2208.04933.
- Sutton, R. S. and Barto, A. G. *Reinforcement learning: An introduction*. MIT press, 2018.
- Sutton, R. S., Precup, D., and Singh, S. Between MDPs and semi-MDPs: A framework for temporal abstraction in reinforcement learning. *Artificial Intelligence*, 112(1-2):181–211, 1999.
- Tassa, Y., Doron, Y., Muldal, A., Erez, T., Li, Y., Casas, D. d. L., Budden, D., Abdolmaleki, A., Merel, J., Lefrancq, A., et al. Deepmind control suite. *arXiv preprint arXiv:1801.00690*, 2018.
- Tessler, C., Givony, S., Zahavy, T., Mankowitz, D., and Mannor, S. A deep hierarchical approach to lifelong learning in minecraft. In *Proceedings of the AAAI Conference on Artificial Intelligence*, volume 31, 2017.
- Williams, R. J. Simple statistical gradient-following algorithms for connectionist reinforcement learning. *Machine Learning*, 8:229–256, 1992.
- Yampolskiy, R. V. *Artificial intelligence safety and security*. CRC Press, 2018.
- Ye, W., Liu, S., Kurutach, T., Abbeel, P., and Gao, Y. Mastering atari games with limited data. *Advances in Neural Information Processing Systems*, 34:25476–25488, 2021.
- Zhang, W., Wang, G., Sun, J., Yuan, Y., and Huang, G. Storm: Efficient stochastic transformer based world models for reinforcement learning. *Advances in Neural Information Processing Systems*, 36, 2024.
- Zuo, S., Liu, X., Jiao, J., Charles, D., Manavoglu, E., Zhao, T., and Gao, J. Efficient long sequence modeling via state space augmented transformer. *arXiv preprint arXiv:2212.08136*, 2022.

605 **A. Background**

606 **A.1. Learning a World Model in DreamerV3**

608 Our method is build on top of DreamerV3 (Hafner et al., 2023). DreamerV3 learns a world model in a latent space in order
609 to increase efficiency:

610
$$(h_t, z_t) = \text{RSSM}(h_{t-1}, a_{t-1}, o_t) \quad (13)$$

613 with h_t being the deterministic part of the latent state and z_t being the stochastic part of the latent state. The world model is
614 trained to predict the next latent state (h_{t+1}, z_{t+1}) given the world model state (h_t, z_t) and the current action a_t . Specifically,
615 the world model learns a distribution $p_\theta(z_t|h_t, o_t)$ predicting the stochastic state from the last deterministic state and an
616 observation o_t and another distribution $q_\theta(z_t|h_t)$ predicting the stochastic state purely from the last deterministic state. q_θ is
617 used during imagination. It then predicts the reward r , the continue signal c and the decoded observation o given the current
618 world state, which enables DreamerV3 to train an actor critic entirely on imagined trajectories in latent space. The world
619 model is trained with a loss function that is a weighted sum of the loss of the dynamic, observation, continue, and reward
620 prediction.

621 The RSSM dynamic prediction model uses a GRU (Cho et al., 2014) to predict the next deterministic state h_{t+1} and a
622 discrete categorical distribution to sample z_{t+1} . There are several works that replace the GRU with different, more complex
623 models (Chen et al., 2022; Robine et al., 2023; Deng et al., 2023).

625 For imagining the trajectories, the world model starts with an initial observation o_0 and an initial state h_0 . It then computes
626 the first world state (h_0, z_0) . The agent interacts with this model, which simulates the original environment:

627
$$a_t = \pi(h_t, z_t) \quad (14)$$

628
$$(h_{t+1}, z_{t+1}) = \text{RSSM}(h_t, a_t, z_{t+1}) \quad (15)$$

631 **A.2. Hierarchical Reinforcement Learning**

633 Hierarchical models have been shown to be a powerful tool in RL (Dayan & Hinton, 1992; Parr & Russell, 1997; Sutton
634 et al., 1999). The idea is to break down a complex task into easily achievable subtasks. This subtask definition can be done
635 manually (Tessler et al., 2017) or automatically (Li et al., 2022; Nair & Finn, 2019; Kujanpää et al., 2023). This typically
636 involves learning a high level actor that works at larger timescale and a low level actor that executes proposed subgoals
637 (Hafner et al., 2022a; Nachum et al., 2018; Jiang et al., 2019; Nachum et al., 2019a):

638
$$g_t = \pi_{high}(s_t) \quad (16)$$

639
$$a_t = \pi_{low}(s_t, g_t) \quad (17)$$

642 with s_t being the current environment state, g_t being the proposed subgoal and a_t being the action taken by the low level
643 actor. The low level actor is often encouraged to fulfill the subgoal by adding a subgoal reward r_g to the extrinsic reward
644 r_{extr} . This subgoal reward is often a function of the distance between the current state and the proposed subgoal (Hafner
645 et al., 2022a; Nachum et al., 2019a).

646 **A.3. Structured State Space Sequence Models**

648 Structured state space sequence models (S4) were initially introduced by Gu et al. (2022) as a sequence modeling method
649 that is able to achieve superior long-term memory tasks than Transformer-based models while having a lower runtime
650 complexity ($O(n^2)$ for the attention mechanism of Transformers and $O(n \log n)$ for S4, n being the sequence length). State
651 Space models are composed of four matrices: A , B , C and D . They take in a signal $u(t)$ and output a signal $y(t)$:

653
$$x(t+1) = Ax(t) + Bu(t) \quad (18)$$

654
$$y(t) = Cx(t) + Du(t) \quad (19)$$

656 with $x(t)$ being the state of the model at time t . The matrices A , B , C , and D are learned during training. Gu et al.
657 (2022) propose various techniques to increase stability, performance and training speed of these models in order to model
658 long sequences. They utilize special HIPPO initialization matrices for this. Another major advantage of S4 layers over
659

660 Transformer models is, besides their better runtime efficiency, that they can be used both as a recurrent model, which
 661 allows for fast autoregressive single step prediction, and as a convolutional model, which allows for fast parallel sequence
 662 modelling. [Smith et al. \(2023\)](#) propose a simplified version of S4 layers (S5) that is able to achieve similar performance
 663 while being more stable and easier to train. Their version utilizes parallel scans and different matrix initialization in order to
 664 further boost the parallel sequence prediction and runtime performance. [Lu et al. \(2023\)](#) propose a resettable version of S5
 665 layers, which allow resetting the internal state $x(t)$ during the parallel scans, in order to apply S5 layers in a RL setting
 666 where the state input sequence might span episode borders.
 667

668 B. Further Related Work

669 B.1. Hierarchical Reinforcement Learning

670 Hierarchical reinforcement learning (HRL) is a field of RL that breaks down complex tasks in time and state abstracted
 671 subproblems on multiple time scales ([Hutsebaut-Buysse et al., 2022](#); [Sutton et al., 1999](#)). This allows the agent to learn
 672 subtasks on different time scales and to reuse these subtasks in different contexts. This is especially useful in sparse reward
 673 environments, where the agent can learn subtasks that are easier to solve and then combine them to solve the overall task
 674 ([Nair & Finn, 2019](#)). [Nachum et al. \(2019c\)](#) show that one of the main benefits of HRL is improved exploration, more than
 675 inherent hierarchical structures of the problem task itself or larger model sizes. [LeCun \(2022\)](#) argue that HRL is a promising
 676 direction for future research in RL, as complex dependencies often are only discoverable by abstraction, as learned skills are
 677 often reusable in different contexts. Also, they show that HRL has deep rooting in human cognition.
 678

679 Goal-conditioned HRL ([Florensa et al., 2017](#); [Nachum et al., 2018; 2019b;a](#)) is a subfield of HRL that uses goal-conditioned
 680 policies to learn subtasks. The agent learns a policy that takes a goal as input and outputs actions that lead to the goal. The
 681 agent can then learn a policy that takes a goal as input and outputs a subgoal that leads to the goal. This allows the agent to
 682 learn subtasks on different time scales and to reuse these subtasks in different contexts. The higher order policy proposes
 683 subgoals in frequent intervals that the lower order policy has to fulfill, which is often incentivized by giving an intrinsic
 684 reward to the lower level policy ([Hafner et al., 2022a](#); [Rosete-Beas et al., 2023](#)). [Hafner et al. \(2022a\)](#) combine a hierarchical
 685 policy with a world model, building on the DreamerV2 architecture ([Hafner et al., 2022c](#)). They show that the combination
 686 of a hierarchical policy and a world model outperforms the original DreamerV2 model on several tasks. The low level policy
 687 receives only subgoal rewards in this architecture, while the higher level policy receives the actual task reward. This is
 688 similar to our approach, but we use a different architecture for the world model, and we let the higher level policies learn a
 689 separate world model.
 690

691 [Gumbesch et al. \(2023\)](#) deploy a hierarchy of world models with a look ahead trajectory search approach called THICK. The
 692 higher level world model is only updated if there are significant changes in the lower level world model states. This allows
 693 their higher level representation space to be highly informative, interpretable and temporally abstract. The time adaptive
 694 character lets THICK capture patterns in the environment over arbitrary time spans. However, they do not deploy single step
 695 predictive actor networks as e.g. Hieros, DreamerV3 ([Hafner et al., 2023](#)) or IRIS ([Micheli et al., 2023](#)) use it, which makes
 696 THICK not directly comparable with the other approaches discussed in our paper.
 697

698 B.2. World Models

700 Environment interactions are typically expensive to train an RL agent. E.g., in robotic applications it is impossible to let the
 701 agent interact with the real environment, as this would be too expensive and potentially dangerous. Therefore, it is desirable
 702 to train the agent in a simulated environment ([Ha & Schmidhuber, 2018](#); [Poudel et al., 2022](#); [Hafner et al., 2020; 2022c;](#)
 703 [2023; 2022b](#)). [Ha & Schmidhuber \(2018\)](#) introduced learning an RNN-based model of the environment and using this
 704 model to train the agent. This allows the agent to learn from simulated data, which is much cheaper than learning from real
 705 environment interactions and can in principle be generated in an infinite amount. [Hafner et al. \(2020\)](#) introduced Dreamer, a
 706 model-based RL agent that learns a world model based on PlaNet ([Hafner et al., 2022b](#)) and uses this world model to train
 707 the agent. PlaNet uses an RNN architecture which predicts the next world state from the last world state and the next action
 708 from the learned policy. It uses an RNN-based architecture. To increase computational efficiency, all learning is done in a
 709 compact latent state. They show that Dreamer outperforms state of the art model-free RL agents on several tasks.
 710

711 [Hafner et al. \(2022c\)](#) introduced DreamerV2, an improved version of Dreamer featuring a discrete stochastic latent state.
 712 They show that DreamerV2 outperforms Dreamer on several tasks. With DreamerV3 ([Hafner et al., 2023](#)) they propose
 713 some additional improvements with which they were able to solve the Minecraft Diamond challenge ([Kanitscheider et al.,](#)

715 2021) without any pretraining. DreamerV3 still uses a PlaNet-based world model, but the model states are composites of a
716 discrete valued stochastic and a continuous valued deterministic part.

717 Several authors propose improvements to this architecture, mostly by proposing improvements to the used world model.
718 Chen et al. (2022) propose replacing the RNN with a Transformer model that takes in a context $(s_0, a_0), \dots, (s_n, a_n)$ of
719 state action pairs (s_i, a_i) in order to compute the next world state. Robine et al. (2023) propose a similar architecture,
720 but in contrast to the previous work, the Transformer model is not used during inference, which makes their model more
721 computationally efficient. Deng et al. (2023) propose S4WM, utilizing S4 layers for the next state prediction. Since S4
722 layers can be used both for predicting sequences in parallel and predicting only the next value in an RNN like fashion,
723 their model also proved to be more computationally efficient than the Transformer-based architectures and outperforms
724 them in memorization capabilities. Agarwal et al. (2023) use Transformer style networks for both world modelling and
725 actor networks. Their architecture takes a history of past world states and predicts the next action from that sequence of
726 so-called world tokens. On the Atari100K benchmark, their approach achieves competitive results. Zhang et al. (2024)
727 implement several changes to the TWM architecture, e.g. taking observations, rewards and actions as single tokens for
728 the sequence model prediction or reconstructing the image input without use of the hidden state. Their model STORM
729 achieves state-of-the-art performance on the Atari100k benchmark, which promises that adopting their changes in Hieros
730 might produce even better results.
731

732 We would also like to point out that the model-free SR-SPR recently proposed by D’Oro et al. (2023) achieves superior
733 scores on the Atari100k benchmark by increasing the replay train ratio and regular resets of all model parameters. They
734 tackle the often observed inability of RL agents to learn new behavior after having been already trained for some time in
735 an environment. However, since this approach is not model based and does not train in imagination, we did not include it
736 into our comparison. Nonetheless, scaling the train ratio and employing model resets for the actor/critic or the S5WM of
737 HIEROS are promising directions for future research.
738

739 **C. Full Atari100k Benchmark**

740
741
742
743
744
745
746
747
748
749
750
751
752
753
754
755
756
757
758
759
760
761
762
763
764
765
766
767
768
769

Task	Random	Human	SimPLE	TWM	IRIS	DreamerV3	Hieros (ours)
Alien	228	7 128	617	675	420	959	828
Amidar	6	1 720	74	123	143	139	127
Assault	222	742	527	683	1 524	706	1 764
Asterix	210	8 503	1 128	1 117	854	932	899
BankHeist	14	753	34	467	53	649	177
Battle Zone	2 360	37 188	4 031	5 068	13 074	12 250	15 140
Boxing	0	12	8	78	70	78	65
Breakout	2	30	16	20	84	31	10
Chop.Command	811	7 388	979	1 697	1 565	420	1 475
CrazyClimber	10 780	35 829	62 584	71 820	59 324	97 190	50 857
DemonAttack	152	1 971	208	350	2 034	303	1 480
Freeway	0	30	17	24	31	0	31
Frostbite	65	4 335	237	1 476	259	909	2 901
Gopher	258	2 412	597	1 675	2 236	3 730	1 473
Hero	1 027	30 826	2 657	7 254	7 037	11 161	7 890
JamesBond	29	303	100	362	463	445	939
Kangaroo	52	3 035	51	1 240	838	4 098	6 590
Krull	1 598	2 666	2 205	6 349	6 616	7 782	8 130
KungFuMaster	258	22 736	14 862	24 555	21 760	21 420	18 793
Ms.Packman	307	6 952	1 480	1 588	999	1 327	1 771
Pong	-21	15	13	18	15	18	5
PrivateEye	25	69 571	35	86	100	882	1 507
Qbert	164	13 455	1 289	3 331	746	3 405	770
RoadRunner	12	7 845	5 641	9 109	9 615	15 565	16 950
Seaquest	68	42 055	683	774	661	618	560
Mean	0	100	34	96	105	112	120
Median	0	100	11	50	29	49	56
IQM	0	100	13	46	50	N/A	53
Optimality Gap	100	0	73	52	51	N/A	49

Table 2. Scores of HIEROS and baselines on the Atari100k test suite. Higher scores for Mean, Median and IQM are better. For Optimality Gap, lower scores are better. DreamerV3 does not report the scores for IQM or Optimality Gap. We show the best results for each row in **bold** font.

D. Visualization of Proposed Subgoals

Figure 5 shows the proposed subgoals for one observation in Frostbite and one observation in Breakout.

To give more insight into how Hieros formulates subgoals in different contexts, we show some more subgoals in Figure 6.

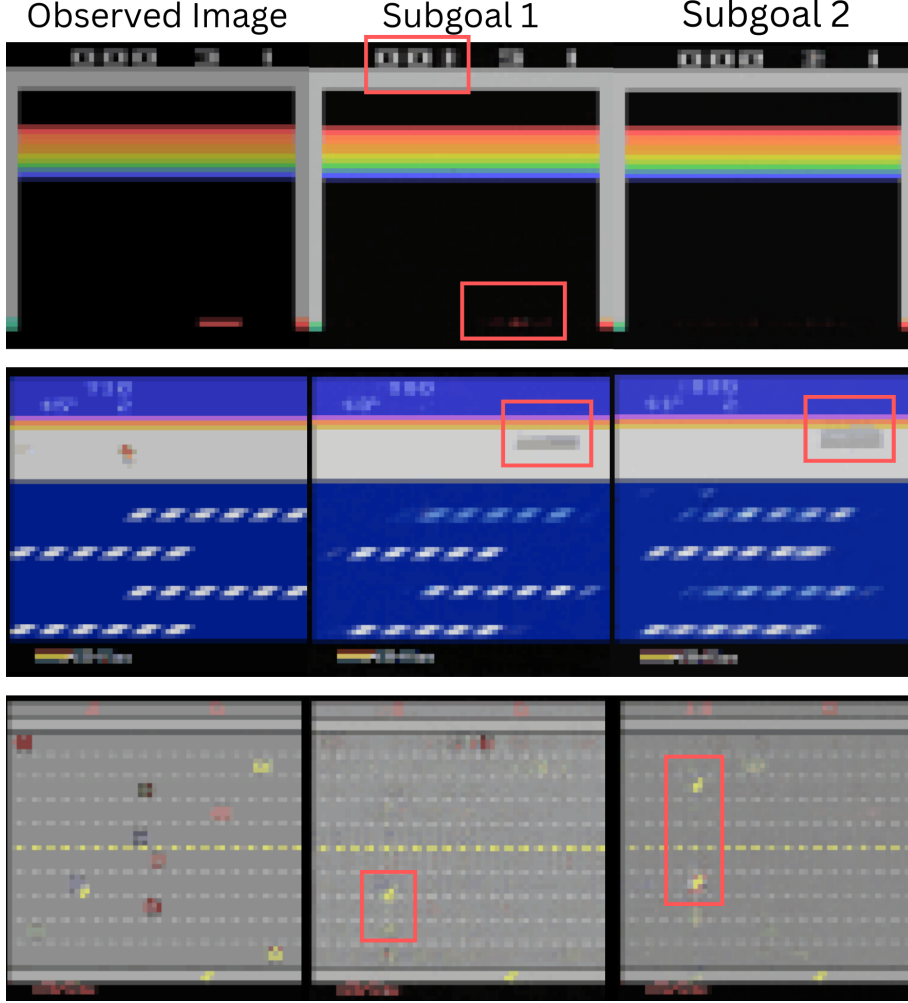


Figure 5. Proposed subgoals for Breakout (top row), Frostbite (middle row), and Freeway (bottom row). The left most frame is the original observation from the environment, and the following frames are the proposed subgoals from the higher level actor. For Breakout, the subgoals are only to increase the level score (marked with the red rectangles) and the ball is not simulated at all, while for Frostbite the subgoals guide the actor towards building up the igloo in the upper right part of the image in order to advance to the next level (red rectangles). For Freeway, which also features a single level and sparse rewards, the subgoals are much more meaningful than for Breakout and guide the actor to move across the road (red rectangles).

E. Hyperparameters

F. Computational Resources and Implementation Details

In our experiments we use a machine with an NVIDIA A100 graphics card with 40 GB of VRAM, 8 CPU cores and 32 GB RAM. Training HIEROS on one Atari game for 100k steps took roughly 14 hours in our setup.

We base our implementation on the Pytorch implementation of DreamerV3 (NM512, 2023) and on the Pytorch implementation of the S5 layer (C2D, 2023). As this version does not implement the resettable version of S5 and Lu et al. (2023) do not provide an open source implementation of their method, we implemented the reset mechanism ourselves in the provided source code. The source code is publicly available under the following URL: <https://anonymous.4open.science/r/Hieros-7C37/>

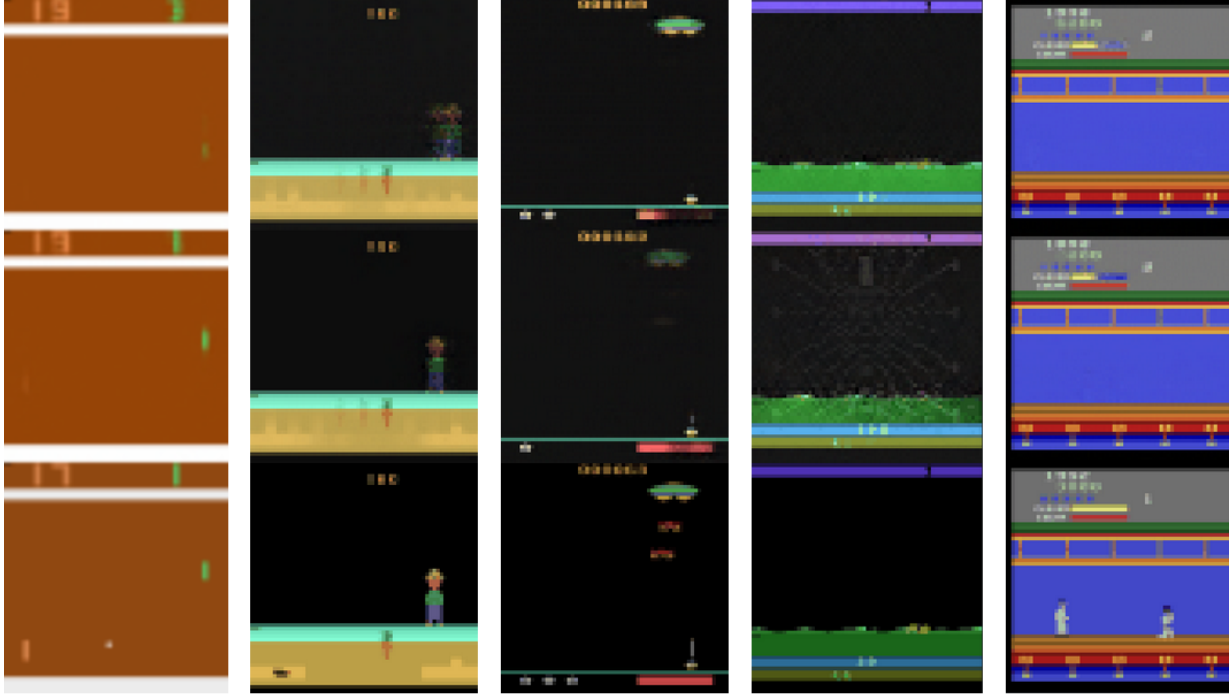


Figure 6. Proposed subgoals for (from left to right) Pong, Gopher, Assault, Krull and Kung Fu Master. The bottom row is the actual observation, the middle row the proposed subgoal from subactor 1 and the top row the proposed subgoal from subactor 2.

G. Ablations

In the following, we provide additional ablation studies exploring the effect of different components of HIEROS. We conduct all ablations on four games: (i) Krull, a game that features multiple levels, (ii) Breakout, a game with a single level and simple dynamics, (iii) Battle Zone, a game with a single level and complex hierarchical dynamics and (iv) Freeway, a game with difficult exploration properties (Micheli et al., 2023). We use the same hyperparameters as described in Appendix E for all ablations. We show the collected reward of the lowest level subactor of HIEROS with S5WM and all hyperparameters as specified in Appendix E in red and the collected reward of HIEROS with the ablation in blue. We use the same color scheme for all ablation studies, except those where the graphs contain more than two lines. We conducted three training runs for each ablation, and the graphs illustrate the average performance across those runs as a line. The shaded area around the line, in the same color, represents the range of values observed during the three runs. In every interaction with the environment, the actor’s action is repeated for four frames, aligning with the methodology adopted in other papers such as Hafner et al. (2022c; 2023); Micheli et al. (2023); Robine et al. (2023). Consequently, the plots display results up to 400k steps, but it’s important to note that only 100k interactions were actually conducted in the specified environments due to the frame repetition.

G.1. S5WM vs. RSSM

In Section 3.2, we compare the model losses and partial rewards of HIEROS in the game of Krull and Breakout using either RSSMs or S5WMS as world models. In Figure 7, we compare the collected rewards of HIEROS using either RSSMs (blue) or S5WMS (red) for Krull, Breakout, Battle Zone, and Freeway against each other. The RSSM is not able to achieve the same performance as the S5WM for Krull, Battle Zone and Freeway. However, for Breakout, the RSSM exhibits a slight improvement compared to the S5WM. This aligns with the observation made in Section 3.2, where it was noted that the world model losses for Breakout were lower when employing an RSSM as the dynamics model compared to using the S5WM.

935	Training parameters:	
936	learning rate	10^{-4}
937	weight decay	0
938	optimizer	AdamW
939	learning rate scheduler	None
940	warmup episodes	1000
941	ETBS temperature τ	0.3
942	batch size	16
943	trajectory length for training	64
944	imagination horizon	16
945		
946	Hierarchy parameters:	
947	hierarchy layers	3
948	subgoal proposal intervals k	4
949	extrinsic reward weight	1
950	subgoal reward weight	0.3
951	novelty reward weight	0.1
952	subgoal shape	8x8
953		
954	World Model parameters:	
955	S5 model dimension	256
956	S5 state dimension	128
957	Number of HIPPO-N initialization blocks J	4
958	Number of S5 blocks	8
959	dynamic loss weight a_{dyn}	0.5
960	representation loss weight a_{rep}	0.1
961	h_t dimension	256
962	z_t dimension	32x32
963	MLP units	256
964	g_ψ KL loss weight β	0.5
965		
966	Total parameters	37.1 M
967		
968		
969		
970	G.2. Internal S5 Layer State as Deterministic World State	
971		
972	In Section 2.2, we describe the S5WM, which uses the S5 layer to predict the next world state. In this section, we explore	
973	the effect of using the internal state x_t of the stacked S5 layers of S5WM as the deterministic part of the latent state h_t	
974	instead of the output of the S5 layers. Other comparable approaches that swap out the GRU in the RSSM with a sequence	
975	model usually use the output of the sequence model as h_t (Chen et al., 2022; Micheli et al., 2023; Robine et al., 2023; Deng	
976	et al., 2023). So, testing this ablation provides valuable insight into how the learned world states can be enhanced in order to	
977	boost prediction performance. Figure 8 shows the influence of using the internal state as h_t vs. using the output of the S5	
978	layers as h_t for HIEROS. Using the internal S5 layer state as deterministic world model state seems to boost the performance	
979	for Krull and Battle Zone while having no clear benefit for Breakout and Freeway.	
980		
981	G.3. Hierarchy Depth	
982		
983	In this section, we show the effect of using different model hierarchy depths. We compare HIEROS with S5WM using a	
984	model hierarchy depth of 1, 2, 3, and 4. Figure 9 shows the collected reward of HIEROS with S5WM using a model hierarchy	
985	depth of 1 (purple), 2 (red), 3 (green), and 4 (light blue) for Krull, Breakout, Battle Zone, and Freeway. Most remarkably,	
986	we can see that HIEROS with just one layer achieves significantly better results in Breakout than with two or more subactors.	
987	This indicates that a single layer algorithms, like DreamerV3, Iris, or TWM have a significant advantage over multi-layer	
988	algorithms, like HIEROS in games with no distribution shifts and easy to predict dynamics like Pong or Breakout while	
989	deeper hierarchies showcase a better performance for games with an intrinsic hierarchical structure like Krull.	

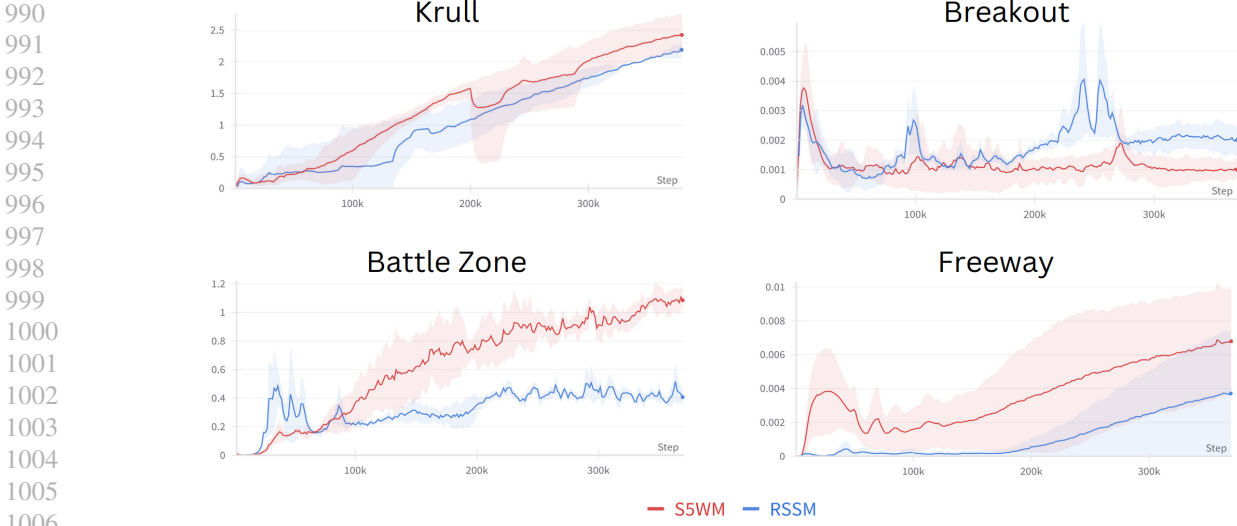


Figure 7. Collected rewards per step for Krull, Breakout, Battle Zone, and Freeway of the lowest level subactor for HIEROS with an RSSM (blue) and HIEROS with an S5WM (red).

G.4. Uniform vs. Time-Balanced Replay Sampling

In Section 2.3, we describe the efficient time-balanced sampling method. In this section, we compare the effect of using uniform sampling vs. our efficient time-balanced sampling for the experience dataset. Figure 10 shows the collected reward of HIEROS with S5WM using uniform sampling (red) and time-balanced sampling (blue) for Krull, Breakout, Battle Zone, and Freeway. As can be seen, in the case of Freeway and Breakout, the time balanced sampling did not provide a significant advantage, while it boosted the performance considerably for Krull and Battle Zone, two games that both display hierarchical challenges. This indicates, that in cases where the model hierarchy can contribute a lot to the overall performance, the actor is more sensitive to overfitting on older training data, containing subgoals produced by less trained higher level subactors.

G.5. Providing k World States vs. Only the k-th World State as Input for the Higher Level World Model

In Section 2.1, we describe how HIEROS provides k consecutive world states of the lower level world model as input for the higher level subactor. However, many approaches such as Director (Hafner et al., 2022a) only provide the k -th world state as input for the higher level world model. In this section, we explore the effect of providing only the k -th world state as input for the higher level world model. Figure 11 shows the collected reward of HIEROS with S5WM using k consecutive world states as input for the higher level world model (red) and only the k -th world state as input for the higher level world model (blue) for Krull, Breakout, Battle Zone, and Freeway. Providing only the k -th world state as input seems to deteriorate the performance for Battle Zone and Freeway while being beneficial for Krull.

G.6. Using a Smaller Version of S5WM

In Section 3.2, we propose a theory that suggests larger S5WM models yield superior results in complex environments, whereas smaller dynamic models may be more advantageous in simpler dynamic environments such as Breakout. In Figure 12, we compared HIEROS using the standard-sized S5WM (in red) with HIEROS using a smaller S5WM, which consists of only 4 S5 blocks and is thus half the size (in blue). In the case of Battle Zone, a game characterized by complex dynamics, the larger S5WM significantly enhances performance. Conversely, for Breakout, we observe that the smaller S5WM performs better during certain stages of training but exhibits a decline towards the end. This suggests that the smaller S5WM could potentially outperform the larger counterpart in this environment, provided additional measures are implemented to prevent actor degeneration during later training stages.

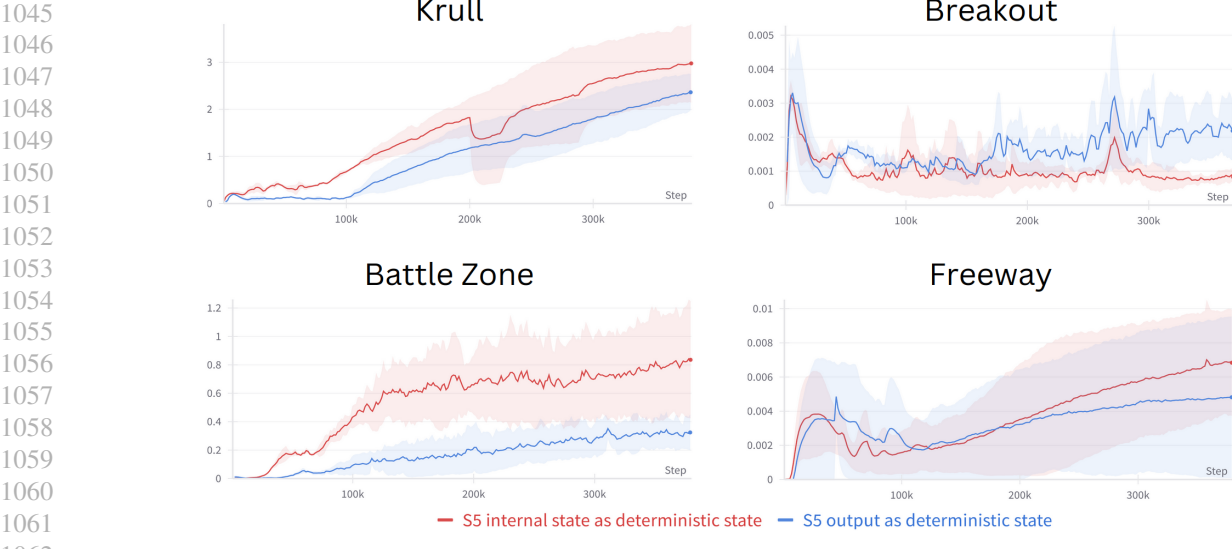


Figure 8. Comparison of the collected reward per step of HIEROS with S5WM using the internal state x_t of the stacked S5 layers as the deterministic part of the latent state h_t (red) and using the output of the stacked S5 layers as h_t (blue) for Krull, Breakout, Battle Zone, and Freeway.

G.7. Providing Decoded Subgoals as Actor Input

In Section 2.1, we explain that in HIEROS, the encoded subgoal g^i from the higher-level policy is passed as input to the lower-level input policy. This differs from the approach in Hafner et al. (2022a), where decoded subgoals from the subgoal autoencoder are passed to the worker policy in their hierarchical model. In Figure 13, we directly compare the impact of using encoded (in red) and decoded (in blue) subgoals as input for the lower-level subactor. Notably, utilizing encoded subgoals appears to enhance performance in Krull and Breakout but leads to a significant degradation in performance for Freeway. In practical terms, a tradeoff must be considered based on the specific environment. It's worth noting that passing decompressed subgoals increases the overall parameter count of the model, but in cases like Freeway, the additional model size contributes to further improvements in rewards.

G.8. Further Ablations Left for Future Work

There are multiple other interesting directions for further ablation studies: One of the main novelties of HIEROS is its use of hierarchical world models. Architectures like Dreamer (Hafner et al., 2022a) however train both the higher and the lower level policy on the same world model, so exploring this might give valuable insights, how much the hierarchical world models contribute to the performance of HIEROS. Another interesting direction is to explore the effect of using differently sized subactors, with the lowest level subactor having the largest amount of trainable parameters and the higher levels having less and less trainable parameters. This could potentially lead to a more efficient use of the available parameters. The higher levels are trained fewer times and with fewer data than the lower levels, so smaller networks might speed up training in those cases.

For HIEROS we relied on the proven world model architecture used by the DreamerV3 model, which features a world state composed of a deterministic and a stochastic part. However, other approaches like IRIS (Micheli et al., 2023) do not rely on this stochastic world state and achieve comparable result. So exploring the effect of using only a deterministic world state might be interesting.

H. CDF of Imbalanced Replay Sampling

In Section 2.3, we use the CDF of the skewed sampling distribution that arises when iteratively adding elements to a dataset and sampling uniformly from it. The distribution is defined as follows:

$$p(x) = \frac{H_n - H_x}{n} \approx \frac{\ln(n) - \ln(x)}{n} = \tilde{p}(x) \quad (20)$$

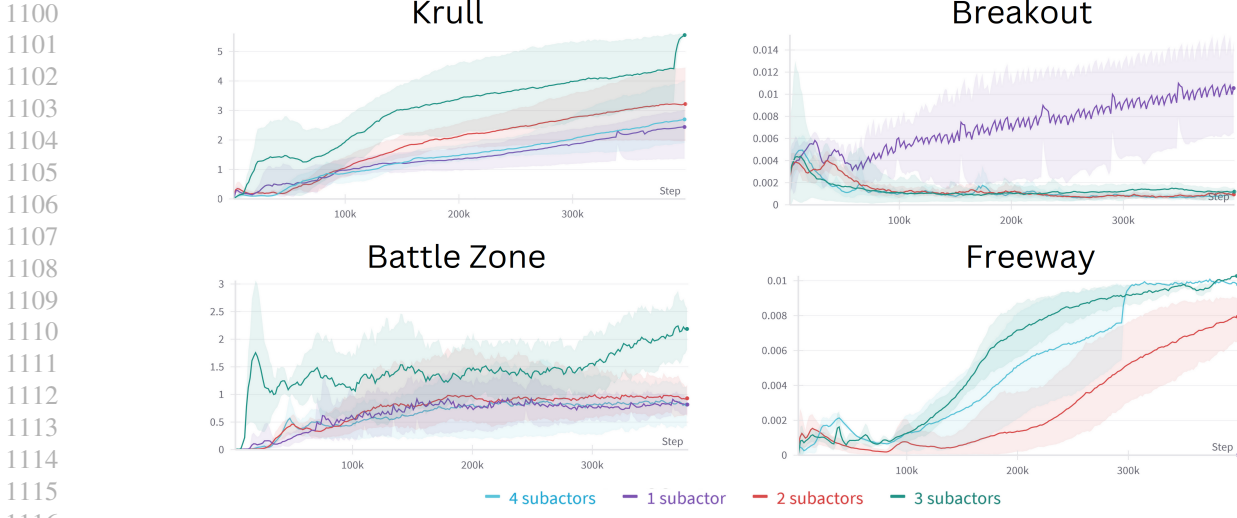


Figure 9. Comparison of the collected reward per step of HIEROS with S5WM using a model hierarchy depth of 1 (purple), 2 (red), 3 (green), and 4 (light blue) for Krull, Breakout, Battle Zone, and Freeway.

with n being the size of the dataset. Since the inequality $\ln(x) < H_x < 1 + \ln(x)$ holds for all $x \geq 2$ we assume without loss of generality that $2 \leq x \leq n$. However, since $\tilde{p}(x)$ does not sum up to 1 over the interval $[2, n]$, we need to divide it by its integral:

$$\begin{aligned} p_s(x) &= \frac{\tilde{p}(x)}{\int_2^n \tilde{p}(x) dx} = \frac{\frac{\ln(n) - \ln(x)}{n}}{\frac{-2 \ln(n) + n + 2 \ln(2) - 2}{n}} \\ &= \frac{\ln(n) - \ln(x)}{-2 \ln(n) + n + 2 \ln(2) - 2} \end{aligned} \quad (21)$$

with p_s being the approximate probability density function of the skewed sampling distribution. The CDF of this distribution is defined as follows:

$$CDF_s(x) = \int_2^x p_s(x) dx = P_s(x) - P_s(2) \quad (22)$$

with $P_s(x)$ being the antiderivative of $p_s(x)$:

$$P_s(x) = \int p_s(x) dx = \frac{x \cdot (\ln(x) - \ln(n) - 1)}{2 \ln(n) - n - 2 \ln(2) + 2} \quad (23)$$

With this, we can derive $CDF_s(x)$ in closed form:

$$CDF_s(x) = \frac{x \cdot (\ln(x) - \ln(n) - 1) + 2(\ln(n) - \ln(2) + 1)}{2 \ln(n) - n - 2 \ln(2) + 2} \quad (24)$$

This can be computed in $O(1)$ time and is therefore very efficient. With the $CDF_s(x)$ we can calculate the efficient time-balanced sampling distribution $p_{etbs}(x)$ as described in Section 2.3. It is also important to mention that we assume, that we only add one item to the dataset and then sample one time after each step. However, if we add k items before sampling s times, the expected number of draws for one element becomes $\mathbb{E}(N_{x_i}) = \frac{k \cdot (H_n - H_i)}{s \cdot n}$. This additional factor $\frac{k}{s}$ is canceled out when computing the probabilities for one element from the expected value, which is why we can ignore this in our computations. Figure 14 shows the sampling counts for different temperatures τ for ETBS.

I. Further Future Work

Another possible future direction would be to use the S5-based actor network proposed by Lu et al. (2023) for HIEROS. Right now, the imagination procedure still relies on a single step prediction of the world model due to the single step

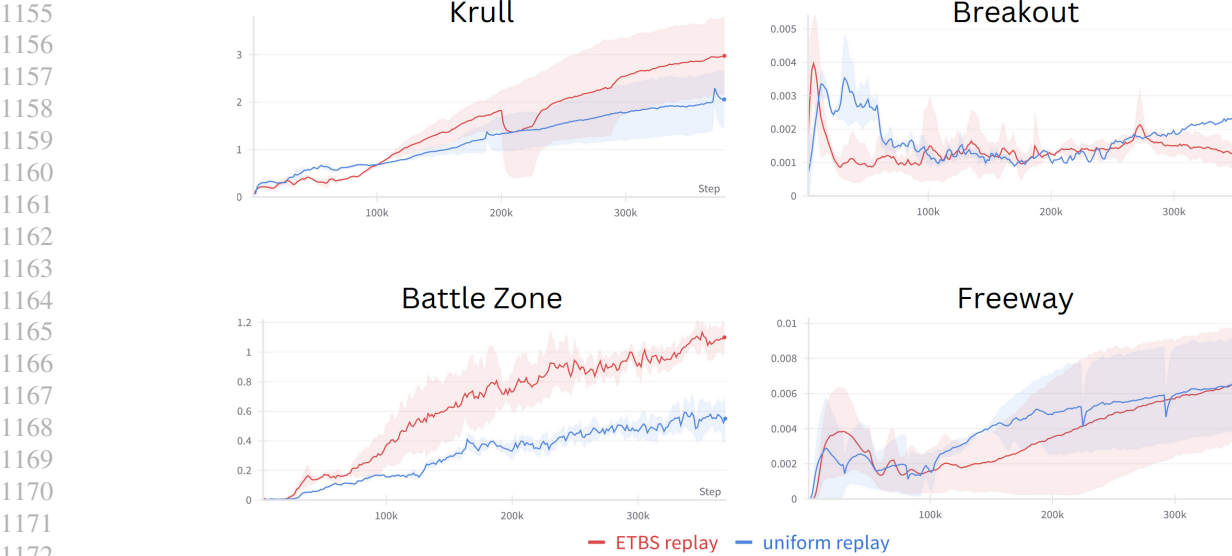


Figure 10. Comparison of the collected reward per step of HIEROS with S5WM using uniform sampling (red) and time-balanced sampling (blue) for Krull, Breakout, Battle Zone, and Freeway.

architecture of the actor network. Using the S5-based actor network would allow for a multistep imagination procedure, which could further improve the performance of HIEROS. This would also open the door to more efficient look-ahead search methods.

Since S4/S5-based models and Transformer-based models show complementary strengths in regard to short and long-term memory recall, many hybrid models have been proposed (Dao et al., 2022; Zuo et al., 2022; Mehta et al., 2022; Gupta et al., 2022). Exploring these more universal models might also be a promising direction for future research.

LeCun (2022) describes a modular RL architecture, which combines HRL, world models, intrinsic motivation, and look-ahead planning in imagination as a potential candidate architecture for a true general intelligent agent. They propose learning a reconstruction free latent space to prevent a collapse of the learned representations, which is already explored in several works for RL (Okada & Taniguchi, 2021; Schwarzer et al., 2021). They also describe two modes of environment interaction: reactive (Mode 1) and using look-ahead search (Mode 2). HIEROS implements several parts of this architecture, namely the hierarchical structure, hierarchical world models and the intrinsic motivation. HIEROS, like most RL approaches, uses the reactive mode, while approaches like EfficientZero (Ye et al., 2021) could be interpreted as Mode 2 actors. Koul et al. (2020) implement a Monte Carlo Tree Search (MCTS) planning method in the imagination of a Dreamer world model. Implementing similar methods for the hierarchical structure of HIEROS, combined with the more efficient S5-based world model (potentially also an S5 based actor network) could yield a highly efficient planning agent capable of learning complex behavior in very dynamic and stochastic environments.

Since Figure 9 demonstrates that for some environments a deeper hierarchy can deteriorate performance, a possible future research could include an automatic scaling of the hierarchy depending on the current environment. E.g. if the accumulated reward stagnates and the agent cannot find a policy that further improves performance, the agent might automatically add another hierarchy layer, perform a model parameter reset and retrain on the collected experience dataset.

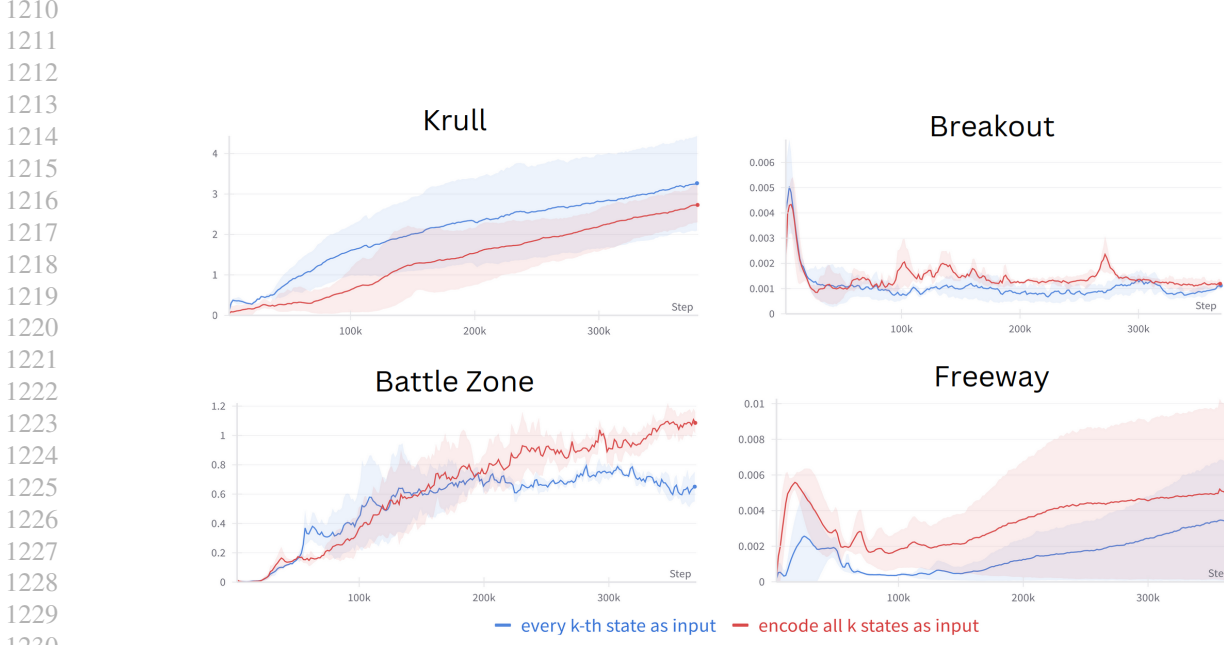


Figure 11. Comparison of the collected reward per step of HIEROS with S5WM using k consecutive world states as input for the higher level world model (red) and only the k -th world state as input for the higher level world model (blue) for Krull, Breakout, Battle Zone and Freeway.

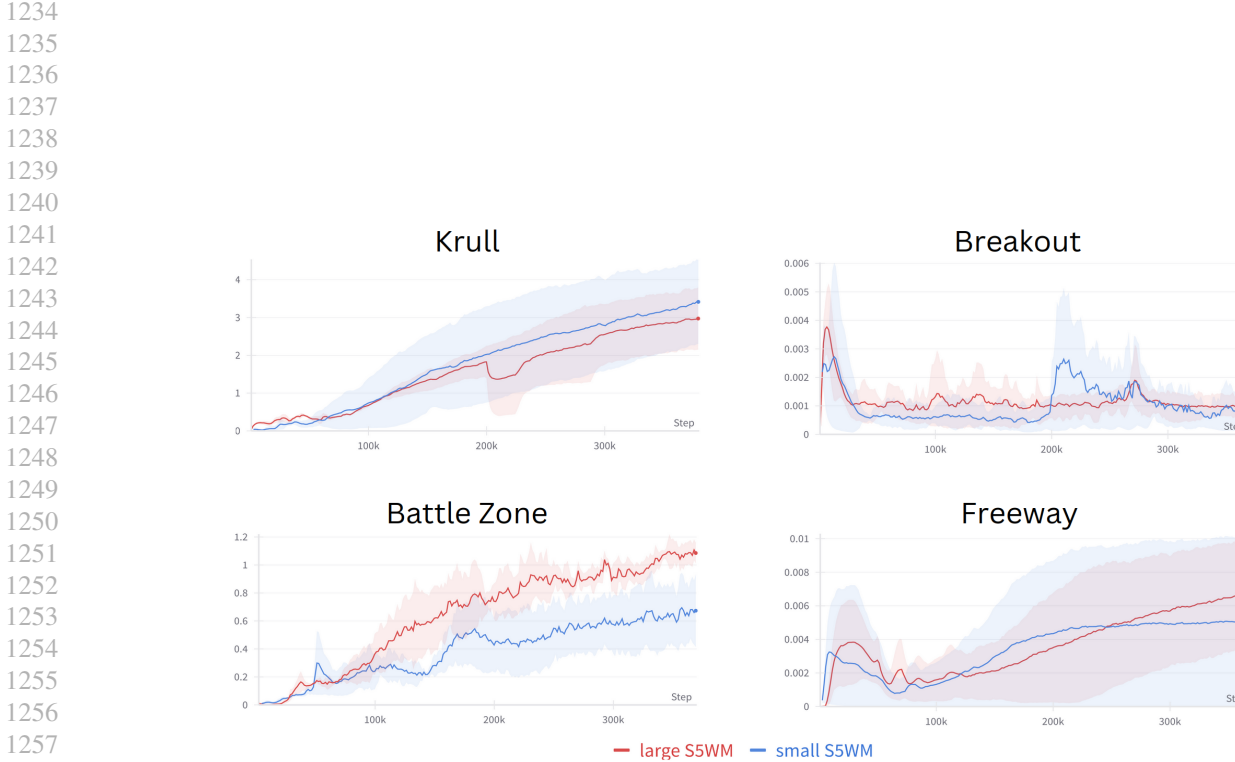


Figure 12. Comparison of the collected reward per step of HIEROS with the standard S5WM (red) and HIEROS using a smaller version of S5WM (blue) for Krull, Breakout, Battle Zone and Freeway.

1261
1262
1263
1264

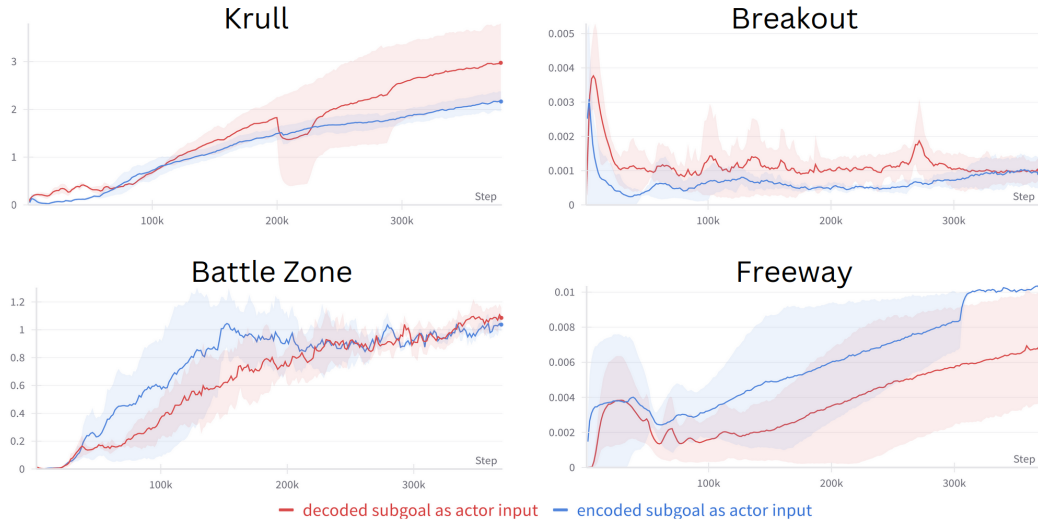


Figure 13. Comparison of the collected reward per step of HIEROS when passing encoded (red) and when passing subgoals decoded by the subgoal autoencoder (blue) to the lower level subactors for Krull, Breakout, Battle Zone and Freeway.

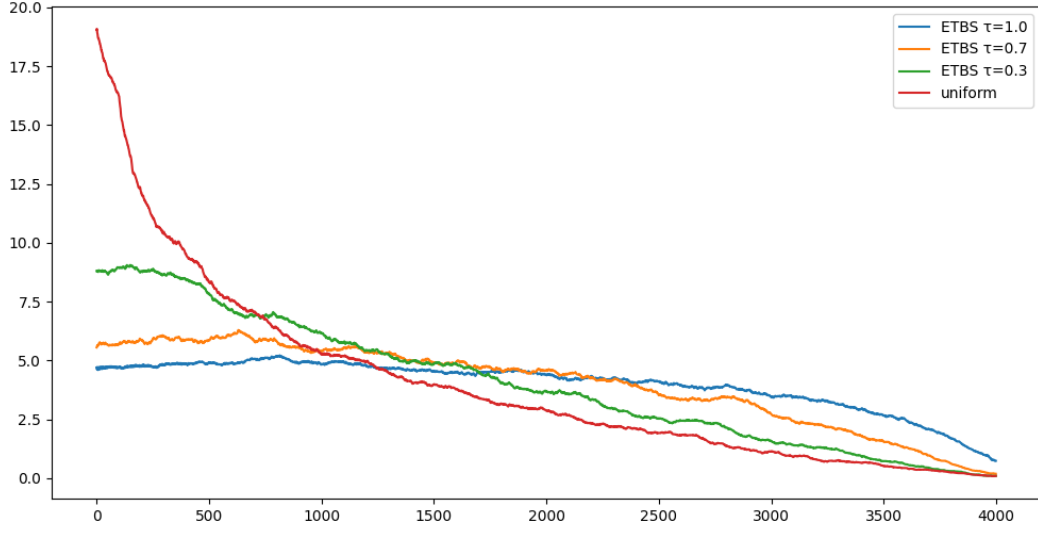


Figure 14. The number of times an entry i is sampled in a dataset of final size 4000 with iteratively adding one element to the dataset and sampling over the dataset afterwards. Compared are the original uniform sampling method implemented in DreamerV3 (Hafner et al., 2023) and our proposed ETBS with different temperatures τ . For our final experiments, we use a temperature of $\tau = 0.3$.